Journal of Structural Geology, Vol. 15, Nos 3–5, pp. 571 to 591, 1993
Printed in Great Britain

0191-8141/93 $06.00+0.00

Geometry and kinematics of continental basement deformation during the Alpine orogeny, Mt. Olympos region, Greece

E. R. SCHERMER

Department of Geology, Western Washington University, Bellingham, WA 98225, U.S.A.

(*Received* 16 *January* 1992; *accepted in revised form* 6 *October* 1992)

Abstract—In the Hellenic Alps, continental crust of the leading edge of the Apulian plate was subducted beneath the European plate during Late Cretaceous–Early Tertiary closure of Tethyan ocean basin(s). Carbonate rocks of the external Hellenides are exposed in the Mt. Olympos tectonic window, overthrust by several thin (~0.2–4 km thick) thrust sheets of granitic basement derived from the internal Hellenides. Field mapping and structural data from the Mt. Olympos region reported here establish the geometry, kinematics and strain history of the continental basement before, during and after continental collision and subduction. Seven deformational events document the change from ductile conditions obtained at depth in the early stages of deformation, to lower temperature ductile and semi-ductile shortening-related fabrics, to brittle extensional features related to exhumation of the metamorphic rocks. D_1–D_4 occurred during subduction of basement nappes and are marked by thrust faulting and folding under blueschist facies conditions; D_5–D_7 are related to unroofing of blueschist facies metamorphic rocks and are associated with extension. Each of the major shortening phases (D_1–D_3) verges toward the foreland (southwest). Oppositely-directed D_5–D_7 extension occurred behind the active thrust belt during continued regional shortening. Normal faults have strongly modified the original thrust-related geometry in the Mt. Olympos region and elsewhere in the internal Hellenides.

INTRODUCTION

THE phenomenon of continental subduction (A-type subduction, Bally 1975) during collisional orogeny was recognized by early workers in the Eastern Alps (Ampferer 1906), and later throughout the Alpine–Carpathian–Balkan chain (e.g. Bernoulli & Laubscher 1972, Burchfiel 1980, Bally 1981). The structural evolution of subducted continental basement is poorly understood because where such terrains are exposed at the surface, (e.g. the Western Alps, Chopin 1984), direct observation of collision-related structures is commonly complicated by late- or post-collisional deformation and metamorphism. In the Mt. Olympos region of the Hellenides, temperatures decreased with time during deformation, leading to preservation of early, subduction- and collision-related high-pressure metamorphic assemblages and structures despite post-collisional tectonism (Schermer *et al.* 1990). In this region then, a detailed analysis of the structures formed during continental subduction is possible.

The Alpine orogeny in Greece was the result of the convergence and collision of the Apulian and European plates during the closure of western Tethys. Ophiolite obduction began in latest Jurassic time (Mercier *et al.* 1975); however, final closure of the ocean basin may not have occurred until latest Cretaceous–Paleocene time (Smith 1971, Bernoulli & Laubscher 1972, Zimmerman & Ross 1976, 1979, Şengör & Yilmaz 1981). Deformation progressed westward from the internal (eastern) Hellenides (Fig. 1), where regional metamorphism and basement-involved thrust faulting occurred during the early stages of the Alpine orogeny, towards the external Hellenides, a thin-skinned fold and thrust belt of Eocene and younger age. Shortening of the Apulian margin has been estimated at 135 km (Zimmerman & Ross 1979) to several hundred kilometers (Bernoulli & Laubscher 1972, Burchfiel 1980).

In the Mt. Olympos region, a cross-section through the transition from the internal to external Hellenides is exposed. The more internal (and structurally higher) nappes record deformation that began in Early Cretaceous time; successively lower and more external nappes, exposed in the Olympos tectonic window (Godfriaux 1968), record Eocene and younger events. The Olympos region is somewhat unusual in that it contains continental basement rocks that were subducted, metamorphosed at high pressure–low temperature conditions and subsequently exhumed (Godfriaux *et al.* 1988, Schermer 1990). Through a detailed study of the geometry and kinematics of structures in the nappe sequence, we can better understand the deformational processes involved in continental collision, subduction, and the uplift and preservation of subducted rocks.

Geologic setting and previous work

The geology of Greece is dominated by NW-trending tectonic belts that formed during the Alpine orogeny (e.g. Aubouin 1959). The Vardar zone, the main oceanic terrane of the Dinaric–Hellenic Alps, contains Middle Jurassic oceanic rocks thought to represent the suture between the Eurasian plate and the Apulian plate (Fig. 1) (Bernoulli & Laubscher 1972, Zimmerman 1972, Mercier *et al.* 1975). Along the western margin of the Vardar zone, ophiolite nappes overthrust the Pelagonian zone (Fig. 1), a metamorphic belt of Paleozoic continental basement rocks overlain by Triassic–Jurassic marble. To the west, Pelagonian rocks overthrust unmetamorphosed Mesozoic and Tertiary carbonates and flysch of the external Hellenides.

The structural sequence in the Mt. Olympos region of

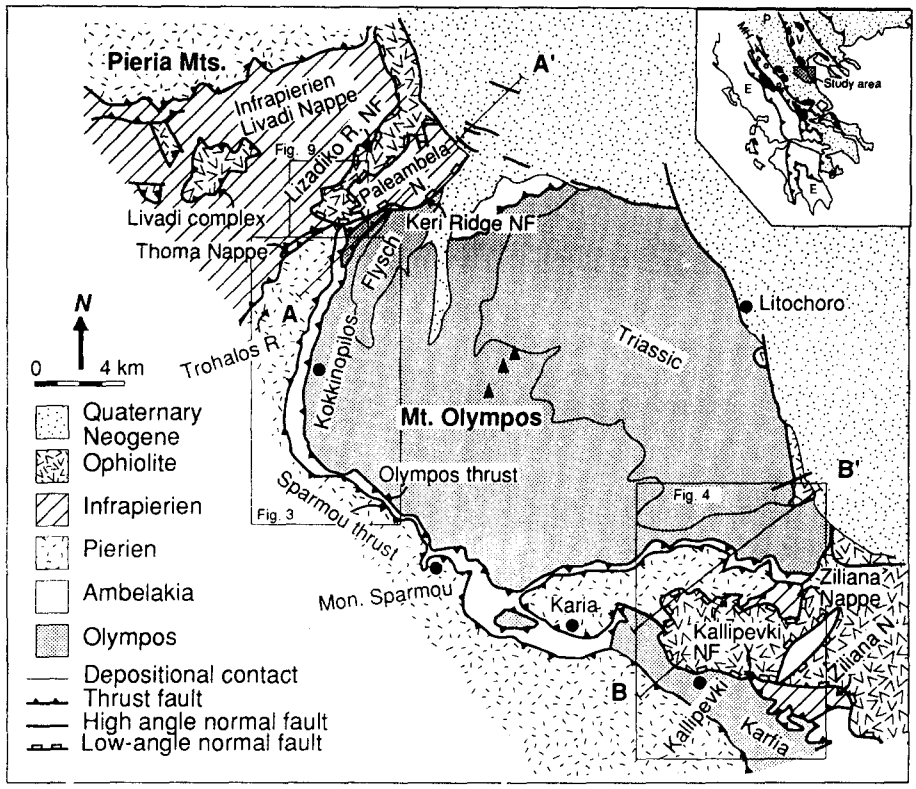

Fig. 1. Generalized geologic map of the Mt. Olympos region, showing principal structural units and the location of Mt. Olympos within the Hellenides (inset). Location of maps in Figs. 3, 4 and 9 indicated by boxes. A–A′ and B–B′ are cross-sections in Fig. 5. Area labelled 'Flysch' indicates location of Eocene flysch of Olympos unit; 'Triassic' indicates location of Triassic carbonate rocks as mapped by Schmitt (1983). Inset: V: Vardar zone; P: Pelagonian zone; MH: Mesohellenic molasse basin; E: External Hellenides. Internal Hellenides are indicated by dot pattern; black areas indicate ophiolites.

the Pelagonian zone, from top to bottom, comprises (Fig. 1; terminology modified from Schmitt 1983): (A) the *ophiolite unit*, consisting of ophiolitic igneous rocks, in coherent thrust sheets and serpentinite–matrix melange, overlain by limestone; (B) the *Infrapierien unit*, gneiss and schist overlain by metasedimentary and metavolcanic rocks and Triassic–Jurassic neritic carbonate rocks; (C) the *Pierien unit*, Paleozoic granitic gneiss overlain by a thin metaclastic sequence and Triassic–Jurassic neritic carbonate rocks; (D) the *Ambelakia unit*, continental margin carbonate and quartzofeldspathic sedimentary rocks, and basic to intermediate volcanic rocks of uncertain age; and (E) the *Olympos unit*, Triassic and Lower Cretaceous to Eocene neritic carbonate rocks overlain by Eocene flysch (Godfriaux 1968, Schmitt 1983).

The ophiolite unit is thought to represent Middle to Late Jurassic oceanic crust that was obducted from one or more Tethyan ocean basins in latest Jurassic to Early Cretaceous time (Hynes *et al.* 1972, Mercier *et al.* 1975, Smith *et al.* 1975, Zimmerman & Ross 1976).

The Infrapierien and Pierien units are interpreted to be parts of the pre-Alpine continental basement and cover sequence, and are referred to by previous workers (e.g. Godfriaux 1968, Papanikolaou 1984a,b) and in this study as the *Flambouron unit* where they are not subdivided. Detailed work in the Olympos region allows internal subdivision of the Pierien and Infrapierien nappes (Fig. 1) (Schmitt 1983, modified by Schermer 1989). Pierien thrust sheets occur above Infrapierien in the Pieria Mountains and below Infrapierien units on the flanks of Mt. Olympos (Fig. 1). Yarwood & Aftalion (1976), Yarwood & Dixon (1977) and Nance (1981) documented the character and age of Cretaceous metamorphism and deformation in the Flambouron unit in the Livadi region and in the Pieria mountains (Fig. 1).

The Olympos unit, undeformed prior to mid-Eocene time, is thought to be a part of the external Hellenides (Godfriaux 1968, Fleury & Godfriaux 1974), and thus the direction of overthrusting of the ophiolite and basement nappes above the Olympos carbonate platform has important implications for the paleogeographic and structural evolution of the Hellenides. Uncertainty about whether the Pelagonian basement was separated from the external Hellenides by an ocean basin or whether it formed the leading edge of the Apulian plate has resulted from controversy over thrust emplacement directions (see Robertson & Dixon 1984, for a review). Stratigraphic correlation suggests SW-directed thrusting (Dèrycke & Godfriaux 1976, Godfriaux 1977, Godfriaux & Pichon 1980). Detailed structural studies of limited portions of the region have been used to postulate NE- (Barton 1975, 1976, Yarwood & Dixon 1977), SE- (Schmitt 1983) and SW- (Vergély 1984, Vergély & Mercier 1990) vergence. The present work attempts to reconcile these conflicting interpretations by considering the thrust system in its regional and temporal context, and by direct examination of kinematic data from thrust-related mylonites.

In this paper I present mapping and structural data

from the Mt. Olympos region which, in conjunction with metamorphic assemblages and radiometric dates reported previously establish the geometry, kinematics and strain history of the continental basement during the Alpine orogeny. The timing of deformation, constrained by cross-cutting relations observed in the field and by absolute age constraints, will be summarized. Microstructural evidence for *P–T* conditions interpreted from deformation mechanisms will be compared with constraints from metamorphic assemblages and Ar/Ar systematics (Godfriaux *et al.* 1988, Schermer 1990, Schermer *et al.* 1990). All geochronological results and metamorphic constraints discussed herein, except where noted otherwise, are from Schermer (1989, 1990) and Schermer *et al.* (1990).

GEOMETRY AND KINEMATICS OF DEFORMATION

Successive deformational events document the change from ductile conditions in the early stages of shortening, to lower temperature ductile and semi-ductile shortening-related structures, to brittle extensional features. In this section I describe the geometry and kinematics of seven deformational events (D_1–D_7; Table 1 and and Fig. 2). Throughout the Pelagonian zone there is evidence for pre-Alpine (pre-Triassic) deformation and amphibolite facies metamorphism (Mercier 1968, Papanikolaou & Zambetakis-Lekkas 1980, Katsikatsos *et al.* 1982, Mountrakis *et al.* 1983), but these events are only locally preserved in the study area (previously called D_0, Schermer *et al.* 1990). The geometry, kinematics, timing and *P-T* conditions of the deformation, combined with regional considerations, suggest that D_1–D_7 are related to convergence between the Apulian and European plates during the Alpine orogeny; D_1–D_4 record shortening associated with continental collision and subduction and D_5–D_7 are related to extension associated with exhumation of the metamorphic rocks from mid-crustal depths (Fig. 5 inset).

The distinction between structures of different deformational events is based on cross-cutting relationships at map to thin section scale, and on the consistency of syn-kinematic metamorphic mineral assemblages related to a given structure or event (Table 1) in cases where style and orientation are not distinctive. Folds and thrusts of D_1, D_2 and D_3 are of similar style and orientation, and all produce penetrative fabrics, as described below. Nevertheless, cross-cutting fabrics and detailed geochronology of minerals formed during the different events, require the presence of three major thrusting events. Moreover, each event D_1–D_3 involves successively younger strata; consideration of the protolith age typically rules out one or more events when assigning relative ages to structures in outcrop (e.g. folds in Eocene flysch cannot be D_1, dated at ~100 Ma). D_4–D_7 did not produce penetrative fabrics, and are distinguished on the basis of structural style and orientation.

D_1: *basement-involved thrusting and folding*

Continental units. The most important distinguishing features of D_1 structures in the field are their association with penetrative moderately high-temperature metamorphic fabrics, the absence of such structures in units younger than the Jurassic marble, and cross-cutting relationships with dated younger structures (e.g. Fig. 3, location 1 shows a D_2 thrust cutting a D_1 thrust). The interpretation that D_1 fabrics formed at greenschist–amphibolite facies at high structural levels and blueschist–greenschist transition facies at lower structural levels derives from extensive petrographic study (which indicates overprinting by two generations of blueschist facies assemblages). Radiometric dating of synkinematic minerals associated with D_1 structures (Fig. 2a) indicates Lower Cretaceous deformation in the Paleambela, Livadi and Thoma nappes (Table 1) and in the Livadi–Pieria region (Yarwood & Dixon 1977).

Characteristics of D_1 deformation include isoclinal folding and imbrication of thin thrust sheets of Pierien and Infrapierien basement granitic gneisses and cover marbles (Table 1, Fig. 2). Thrust sheets range from ~250 to ~4000 m thick (e.g. Thoma nappe, Figs. 1, 3 and 5, C–C′), consist of upper crustal basement rocks (e.g. amphibolite facies pre-Alpine assemblages), and the cover of Mesozoic marbles is typically attached (Fig. 5, B–B′, C–C′). Pierien and Infrapierien units contain a well-developed gneissic layering that is axial planar to F_1 isoclinal folds. F_1 folds are characterized by extreme thinning of the limbs, and hinges are only locally preserved. Fold axes trend NE, parallel to mineral lineations defined by amphiboles and elongate feldspar porphyroclasts. Kilometer-scale recumbent isoclines with axial-planar white micas dated as D_1 occur in the Paleambela nappe (Figs. 1, 2a and 5, A–A′); mesoscopic F_1 folds are scattered due to later deformation (Fig. 6). Poor exposure and overprinting by younger structures makes it difficult to determine the vergence of the large-scale isoclines; small-scale folds verge both northwest and southeast and may be parasitic folds on larger structures.

Along D_1 thrust faults, the S_1 mylonitic fabric is axial planar to large-scale isoclinal folds that fold the thrust fault (e.g. Trohalos ridge, Figs. 1 and 2; Fig. 3, location 2; Fig. 5, C–C′). A well-developed quartz and feldspar elongation lineation within S_1 trends S45–65W, subparallel to the isoclinal fold axes (Fig. 6). The metamorphic assemblages and radiometric dating indicate both the thrust and folds are D_1 in age.

In the Pieria mountains Yarwood & Dixon (1977) attribute ENE- to E-trending mineral lineations and mylonitic foliation to an early deformation phase within the Pierien unit. Later E-trending folds and intersection lineations in underlying Infrapierien amphibolitic and quartzo-feldspathic schists are thought to be related to southward thrusting of the Pierien unit over the Infrapierien unit and the Livadi ophiolite complex (Fig. 1) (Nance 1981, Yarwood & Dixon 1977). Both phases appear to be broadly associated with D_1 (see below).

Table 1. Summary of deformational and metamorphic events

Unit/Event*	Ophiolite	Infrapierien	Pierien	Ambelakia	Olympos	Neogene, Quaternary
D_7	High-angle normal faults	High-angle normal faults	High-angle normal faults	High-angle normal faults	High-angle normal faults	High-angle normal faults
D_6	Open SW folds?	Open SW folds	Open SW folds	Open SW folds	Open SW folds	
D_5 16–23 Ma	Low-angle normal faults	Low-angle normal faults	Low-angle normal faults	Low-angle normal faults	Low-angle normal faults	
D_4		Open NW–SE folds	Close–open NW–SE folds	Close–open NW–SE folds	Open NW–SE folds	
D_3 36–42 Ma			Close-isoclinal NE–SW folds; thrusting to SW Blueschist metamorphism†	Close-isoclinal NE–SW folds; thrusting to SW Blueschist metamorphism†	Close-isoclinal NE–SW folds; thrusting to SW Blueschist–pumpellyite metamorphism†	
D_2 53–61 Ma	? Tight-isoclinal folds, variably oriented Greenschist metamorphism†	Isoclinal NE–SW folds; thrusting to SW Blue-green metamorphism†	Isoclinal NE–SW folds; thrusting to SW Blueschist metamorphism†	Isoclinal NE–SW folds; thrusting to SW Blueschist metamorphism†		
D_1 ≥100 Ma	? Isoclinal folds Greenschist–amphibolite facies metamorphism†	NE to E folds, thrusting to S or SW Greenschist metamorphism†	NE to E folds, thrusting to S or SW Greenschist–amphibolite metamorphism†	? Floating isoclinal fold hinges Blueschist metamorphism†		

*Ages determined from Ar/Ar and Rb/Sr dating (Schermer *et al*, 1990). In the text, folds, fabrics and metamorphic assemblages for a given deformational event are numbered according to the regional D_1–D_7 chronology. For example, D_3 produced F_3 folds, S_3 fabrics and M_3 mineral assemblages, even though within a particular structural unit this may have been the first deformational or metamorphic phase.

†Metamorphism described in more detail in Schermer (1989, 1990).

?—Deformation and metamorphism may not be coeval with the listed event, or may have occurred while the unit was not in contact with other units in the Olympos region. See text for details.

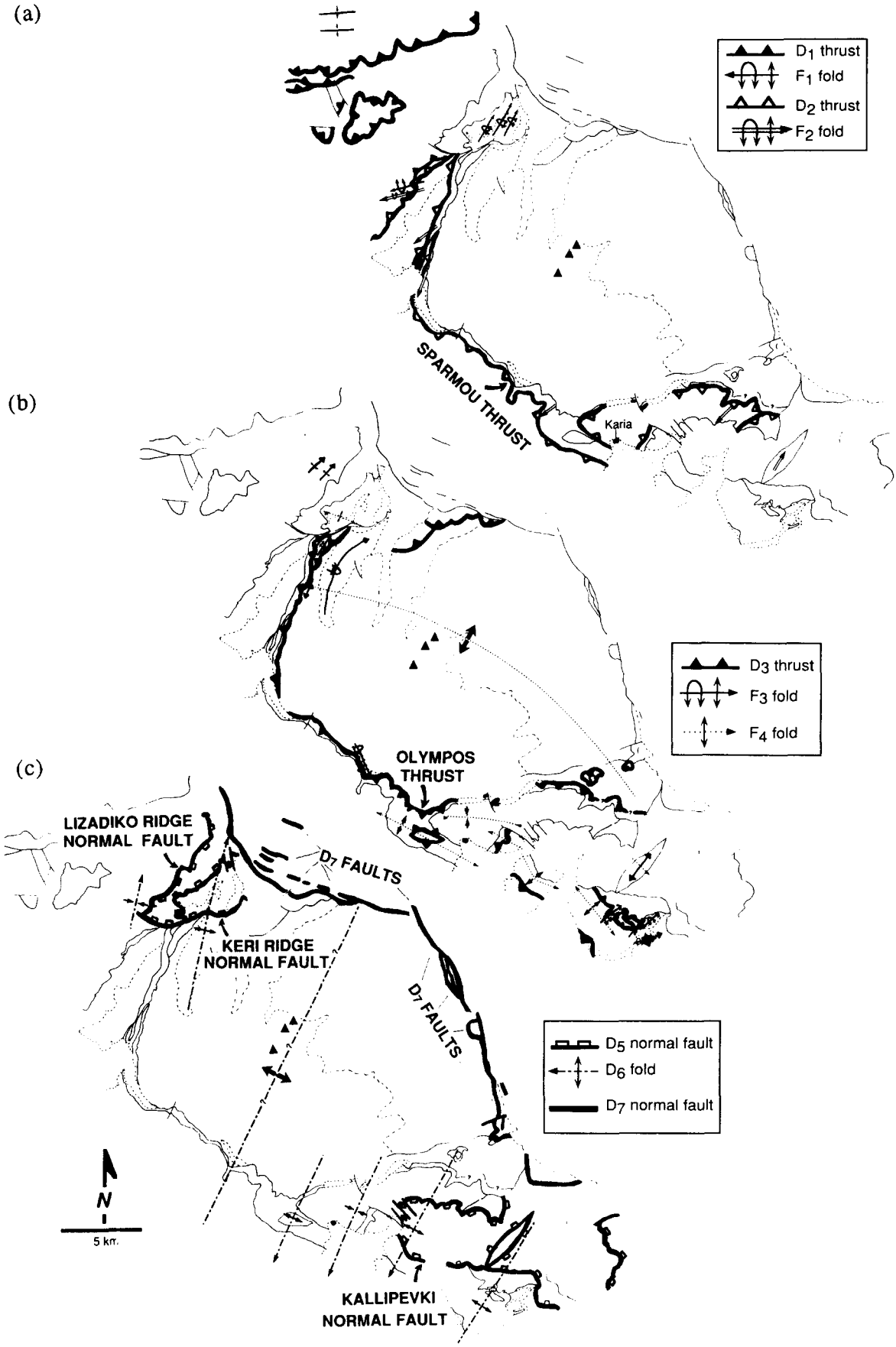

Fig. 2. Tectonic maps of the Olympos region showing folds and faults for events D_1–D_7; all faults are shown by solid lines and all depositional contacts are shown by dashed lines. See Fig. 1 for lithologic unit designations, Table 1 for descriptions, and Figs. 3, 4 and 5 for detailed structural data. In (a), (b) and (c), only the structures for designated deformational events are indicated by heavy lines. (a) Structures developed during D_1 and D_2. (b) Structures developed during D_3 and D_4. (c) Structures developed during D_5, D_6 and D_7.

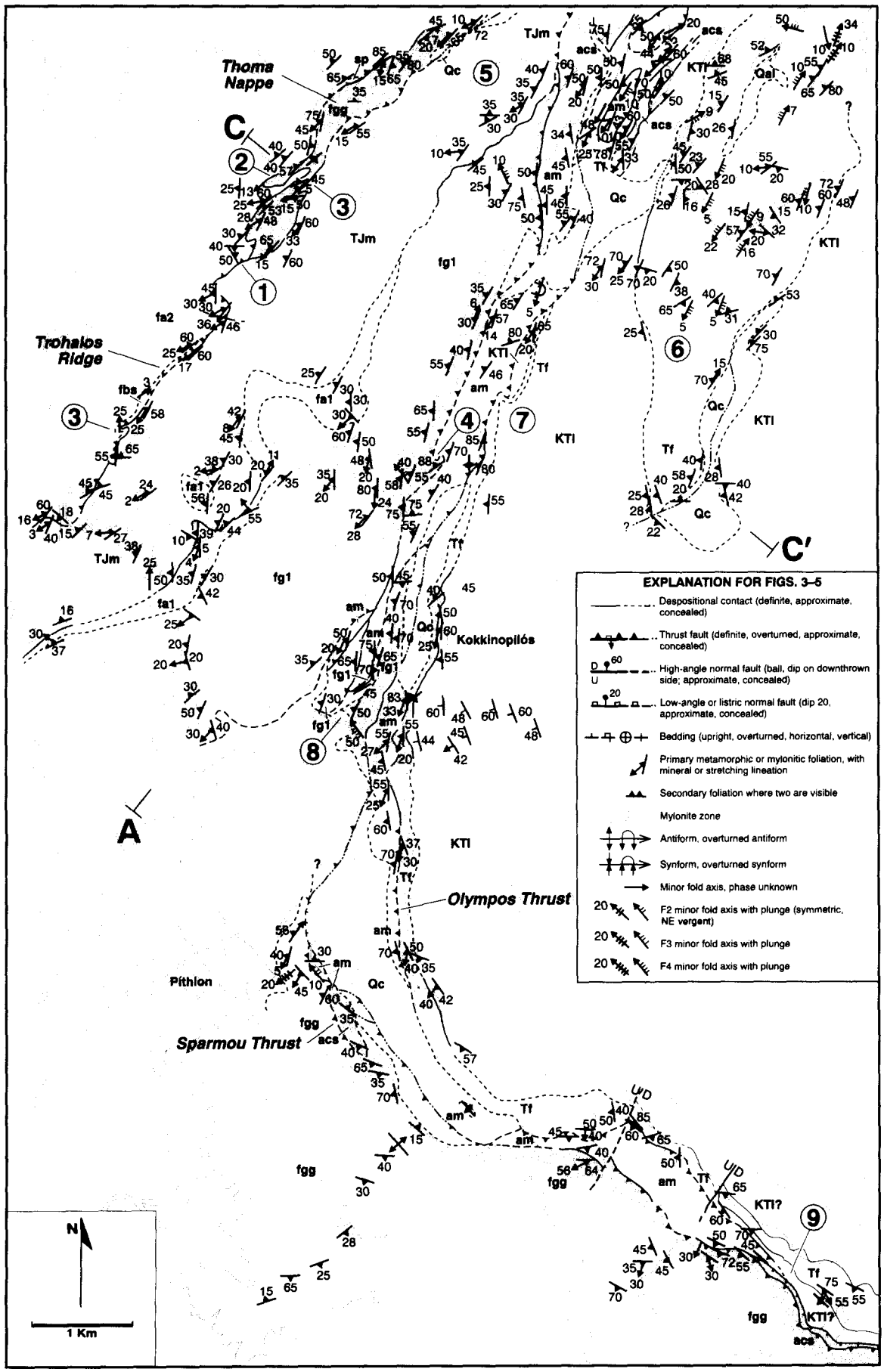

Fig. 3. Geologic map of a portion of the Mt. Olympos region, compiled from 1:25,000 mapping completed by the author, 1983–1986. The location is shown on Fig. 1, and explanation of map units in Fig. 5. Numbers in circles are locations of structural features discussed in the text; some features are shown at more than one location. The locations of the cross-sections in Fig. 5 are shown, note that A′ is off the eastern edge of of the map (see Fig. 1).

Deformation and emplacement(?) *of the ophiolite unit*. Previous workers in the Olympos region have interpreted all contacts at the base of the ophiolite unit as early (i.e. D_1) thrusts related to ophiolite emplacement (e.g. Katsikatsos *et al.* 1982, Schmitt 1983). More detailed study (Nance 1981, this study) suggests that only the Livadi ophiolite complex (Fig. 1) contains structures that, on the basis of similar style, orientation, and grade of associated metamorphism, appear to be spatially and temporally associated with D_1 structures in

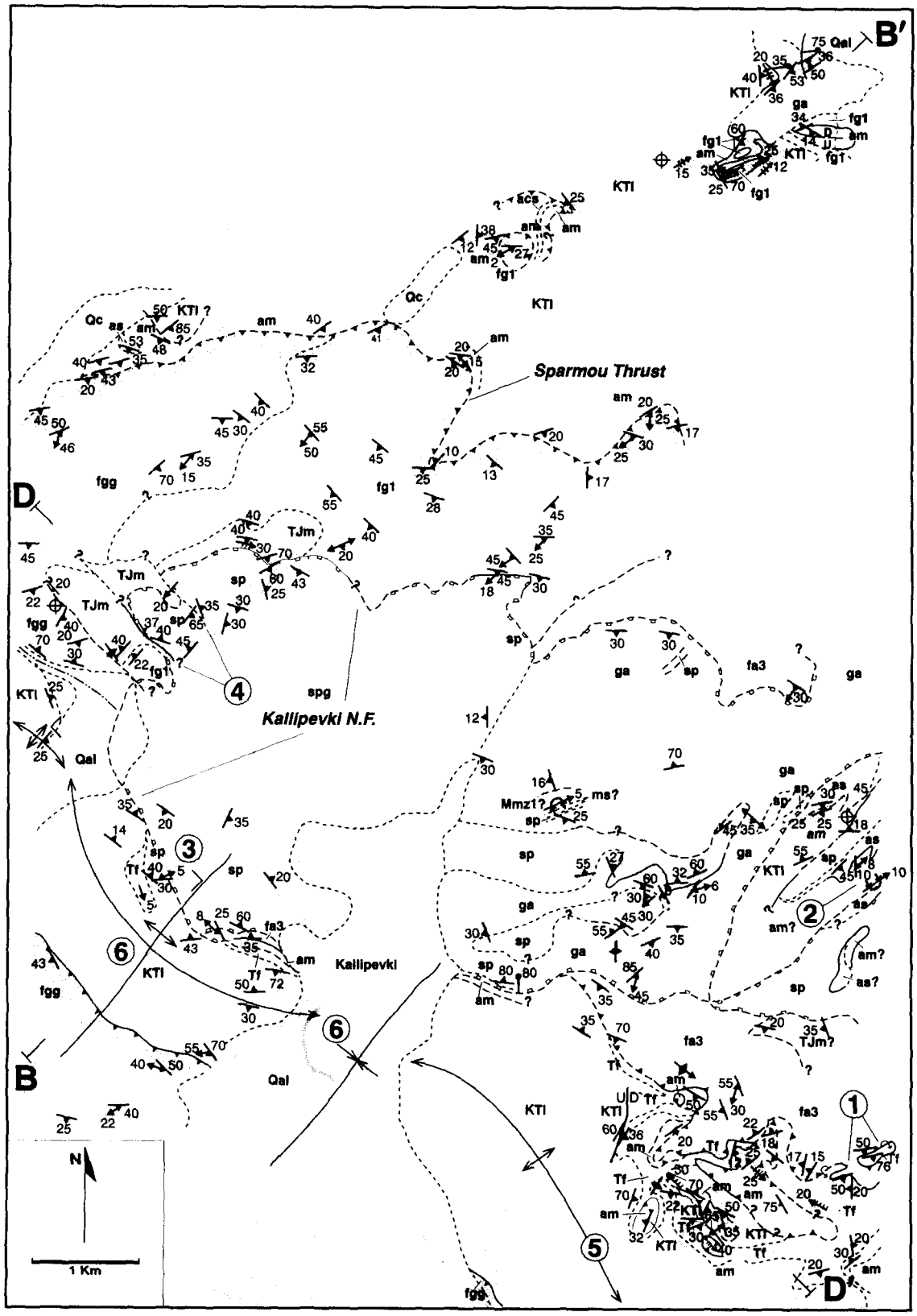

Fig. 4. Geologic map of a portion of the Mt. Olympos region, compiled from 1:25,000 mapping completed by the author, 1983–1986. The location is shown on Fig. 1, explanation of structure symbols on Fig. 3, and explanation of map units on Fig. 5. Numbers in circles are locations of structural features discussed in the text. The locations of the cross-sections in Fig. 5 are shown.

EXPLANATION

QUATERNARY AND NEOGENE

Qal/Qc	Alluvium, scree, covered areas, undivided
Qol	Older, consolidated alluvium
Ngc	Conglomerate, sandstone, marl; probable Neogene age (Godfriaux, 1968)

OPHIOLITE UNIT

Mzm1	Marble, cipolin blocks in melange
cs	calcareous schist, choritic phyllite, psammite
ms	chlorite-phengite schist
sp/spg	serpentinite, serpentinized ultramafic rock, amphibolite, undivided
ga	amphibolite gneiss, schist, gabbro, greenstone

FLAMBOURON--INFRAPIERIEN UNIT
Relative ages below TJm unknown

Paleambela nappe

TJm	Triassic-Jurassic thick-bedded marble
fgs	felsic muscovite-epidote schist, augen schist, gneiss

Livadi Nappe

TJm	Triassic-Jurassic thick-bedded marble
fbs	blue and purple mica schist
fa2	amphibolite gneiss, schist; minor felsic gneiss
fm	marble layers in fa2

Ziliana Nappe

TJm	Triassic-Jurassic thick-bedded marble
fa3	amphibolite schist, gneiss, mica schist, chlorite schist

FLAMBOURON--PIERIEN UNIT
Relative ages below TJm unknown

TJm	Triassic-Jurassic thick-bedded marble
fa1	amphibolite schist, augen schist, mica schist
fg1	granitic and lesser amphibolite gneiss
fgg	granitic gneiss

AMBELAKIA UNIT
relative ages unknown:

as	blue and green mica schist, metabasalt, felsic mica gneiss
am	thin-bedded marble and cherty marble interbedded with blueschist and psammite
acs	calcareous schist, metasandstone, phyllite

OLYMPOS UNIT

Tf	Eocene flysch: sandstone, siltstone, calcareous siltstone, conglomerate
KTl	Upper Cretaceous-Eocene thin to thick bedded limestone

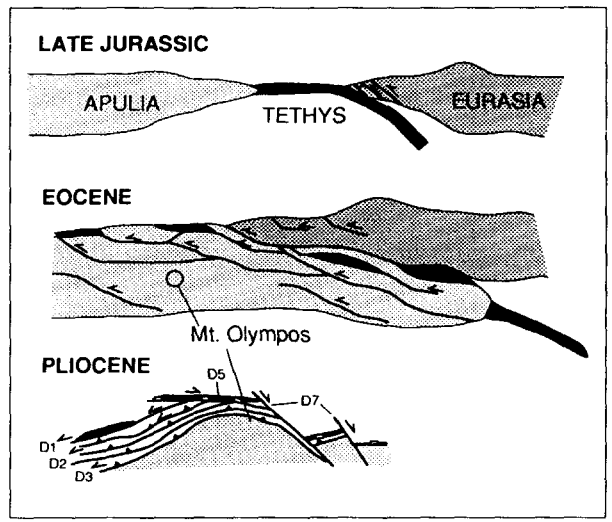

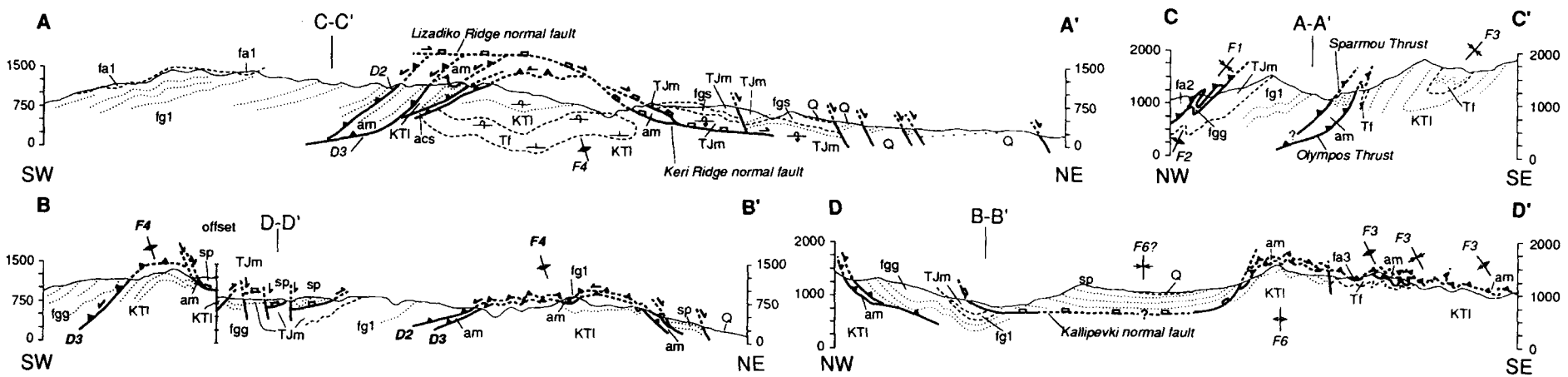

Fig. 5. Explanation of map symbols for Figs. 4, 5 and 7, and geologic cross-sections of the Mt. Olympos region. Cross-section locations A–A′ and B–B′ are shown on Fig. 1; note the offset in section B-B′. The locations of cross-sections C–C′ and D–D′ are shown in Figs. 3 and 4, respectively. Inset shows schematic structural evolution of the region.

the underlying Flambouron units. Probable D_1 structures in the ophiolite unit include epidote–amphibolite facies metamorphic assemblages associated with a variably-developed S_1 foliation, amphibole mineral lineation, and isoclinal folds (Table 1). Nance (1981) described amphibolite facies metamorphism and deformation of the the Livadi complex that produced NE–SW lineation and isoclinal fold axes during initial emplacement above the Infrapierien gneisses. Subsequent deformation produced NE–SW lineations, thrusting within the Flambouron units and Livadi complex, and retrogression to greenschist facies. Similar structures in other ophiolite fragments throughout the study area may be D_1 in age, but the subsequent history differs from that of underlying continental units, and the present contacts below these ophiolitic rocks are brittle structures related to much younger deformation (see D_5). Thus the paleogeographic position and timing of D_1 in the ophiolite unit is uncertain.

D$_1$ *kinematics*. Owing to the localized preservation of D_1 structures in the study area, it is difficult to place

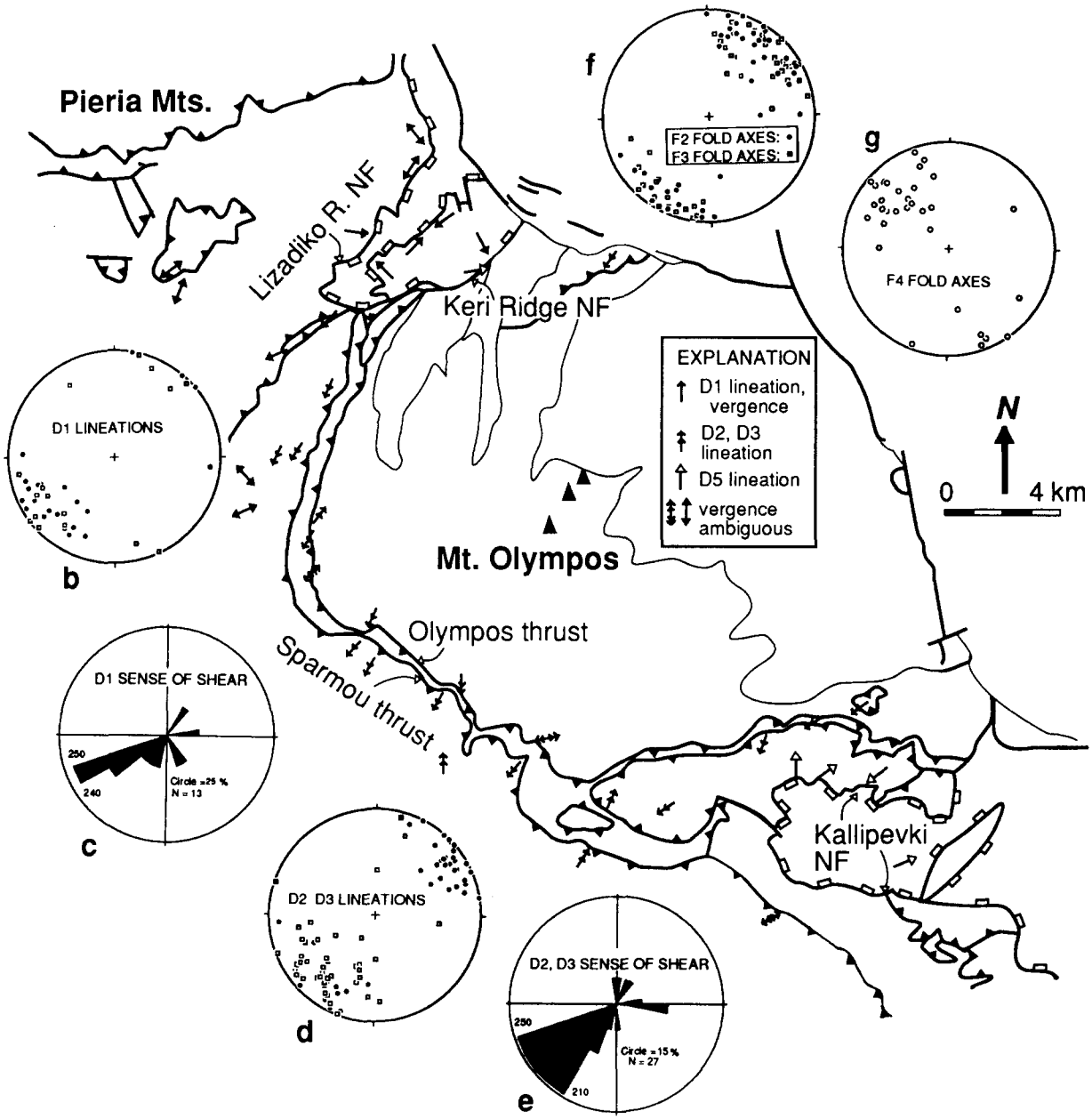

Fig. 6. Map and lower-hemisphere equal-area stereographic projections of kinematic indicators along major faults. (a) Map showing location of oriented samples used to determine sense of shear. Direction of arrow shows direction of movement of the upper plate, inferred from direction of mylonitic stretching lineation and kinematic indicators in outcrop and oriented thin sections. If more than one sample was collected from an outcrop and all gave the same sense of shear, the average direction is plotted on the map. (b) Stereonet plot of L_1 mylonitic lineations adjacent to thrust faults (open squares) and mineral and stretching lineations (closed circles). (c) Rose diagram showing sense of shear as determined from microstructural analyses (see text for explanation). Of 18 samples that contain probable D_1 fabrics, five have poorly-developed or ambiguous fabrics, two show northeast shear sense, two show southeast shear sense, and nine show SW-directed shear. (d) Steronet plot of L_2 and L_3 mylonitic lineations (squares) and mineral lineations (circles). (e) Rose diagram indicating the shear sense for D_2 and D_3 mylonites where it could be determined (27 out of 42 samples). (f) Stereonet plot of F_2 (circles) and F_3 (squares) fold axes from the northwest, west and southwest flanks of Mt. Olympos. (g) Stereonet plot of F_4 fold axes.

independent constraints on the kinematics of this event. Stretching and mineral lineations in oriented samples from mylonitic rocks along D_1 thrusts generally trend NE–SW. The sense of shear, as determined by *S–C* fabrics, asymmetric augen and pressure shadows, and deformation lamellae in quartz (Simpson & Schmid 1983, Lister & Snoke 1984), shows moderately consistent SW-vergence (Figs. 6 and 7a). Oriented samples from the base of the Livadi ophiolite nappe yielded an ambiguous sense of shear, in part because the serpentinites in the upper plate contain a variable lineation and foliation direction, and the quartzo-feldspathic rocks of the lower plate are not well exposed adjacent to the contact. The parallelism between F_1 isoclines and mineral lineations, and the inconsistent vergence of F_1 folds, suggests that the folds may have formed or been rotated parallel to the transport direction (Escher & Watterson 1974), consistent with northeast or southwest transport. Although D_1 kinematic data do not conclusively demonstrate thrust vergence, it will be argued below that a combination of tectonostratigraphic and geochronologic data constrain D_1 thrust faults to have movement directions similar to D_2 and D_3.

Metamorphic and microstructural evidence for P–T *conditions*. In the Pieria Mountains (Fig. 1), where younger events are less penetrative, D_1 structures in Flambouron rocks are associated with greenschist and amphibolite facies metamorphic assemblages (Yarwood & Dixon 1977, Nance 1981, Schmitt 1983, Godfriaux *et al.* 1988). At Mt. Olympos, greenschist facies D_1 assemblages are preserved at high structural levels (Paleambela, Livadi nappes; Schermer 1990).

In mylonite zones along D_1 thrust faults, ribbon quartz and moderately well-developed dynamically recrystallized subgrains and new grains in tails of feldspar augen (Fig. 7a) suggest $T \sim$ 400–500°C (Simpson & DePaor 1991), in agreement with estimates from metamorphic assemblages.

D_1 *timing*. I correlate structures formed during greenschist and higher grade metamorphism in the Pierien and Infrapierien units with D_1 structures that are recognized by previous workers north and west of Mt. Olympos (Yarwood & Dixon 1977, Nance 1981, Schmitt 1983). Because the Triassic–Jurassic marbles are affected by D_1 structures, deformation must be post-Jurassic. The similarity in metamorphic grade of D_1 structures in the Livadi ophiolite complex (Nance 1981) and the Infrapierien (Livadi) unit, suggests these units were juxtaposed during D_1. Other exposures of the ophiolite unit, however, may not have been emplaced until much later, as discussed above.

Radiometric age constraints

Yarwood & Dixon (1977) obtained Rb–Sr internal isochron ages of 119 ± 3 and 116 ± 5 Ma on deformed granitic rocks of the Pierien unit in the Pieria mountains and an Rb–Sr internal isochron age of 101 ± 2 Ma on augen schists from the Infrapierien (Livadi) unit. They interpreted the younger age as a maximum and postulated two distinct events, the first in Early Cretaceous time, and the second in post-Late Cretaceous time. Barton (1976) obtained mica-whole rock ages of 124 ± 4 and 123 ± 11 Ma from mylonitic Pierien granites near Karia, southern Olympos (Fig. 1). Ar/Ar isochron ages of white micas from the Infrapierien (Livadi and Paleambela) unit are 98 ± 2 and 100 ± 2 Ma, and Paleozoic white micas in the Thoma nappe appear to have been reset during mid-late Cretaceous time, supporting occurrence of one or more Cretaceous events (Schermer *et al.* 1990).

D_2 *and* D_3: *basement-involved thrusting under blueschist facies conditions*

D_2 and D_3 are characterized by shortening during basement-involved folding and thrust faulting that occurred at relatively high pressure–low temperature conditions (Table 1; Figs. 2a & b). Blueschist facies mineral assemblages characteristic of D_2–D_3 are observed to overprint greenschist facies assemblages and help to distinguish these events from D_1. The structural style and orientation of D_2 and D_3 are similar and distinguishing the two events is difficult, so I describe them together in this section. Except where F_3 folds are observed to fold the S_2 fabric (Fig. 7c), S_3 cannot be distinguished from S_2 in the basement gneisses, so they are not given separate symbols in Figs. 3 and 4. However, because protolith ages and Ar/Ar ages of synkinematic minerals require two events (Table 1), the structures are separated where possible (Figs. 2a & b) based on the following criteria: locally, small-scale structures from all of events D_1–D_3 are visible in thin section or outcrop (Fig. 7b). Structures that involve the Olympos unit are, by definition, D_3 or younger, structures younger than D_3, however, are much less penetrative and not associated with metamorphic fabrics. I assign to D_2 the Sparmou thrust and all structures adjacent to and clearly geometrically and kinematically associated with that thrust. The thrust is easily traceable in the field as the sheared boundary between Ambelakia unit below and other units above (Fig. 7d). The relative age designation is assigned because (1) deformed Ambelakia unit clastic rocks are considered to be as young as Paleocene in areas south of Olympos (Dèrycke & Godfriaux 1978) and therefore cannot contain Cretaceous D_1 structures, and (2) Ar/Ar ages of mylonitic white micas from several locations along the Sparmou thrust are early Eocene, and thus clearly older than D_3 structures which involve middle Eocene rocks of the Olympos unit.

Continental units.

Infrapierien unit

D_2 and D_3 structures are irregularly developed in the Infrapierien unit. The mylonitic fabric and SW-plunging isoclinal folds associated with the thrust between the Livadi nappe and Pierien marbles on Trohalos ridge cut the D_1 thrust, and fold and transpose S_1. These struc-

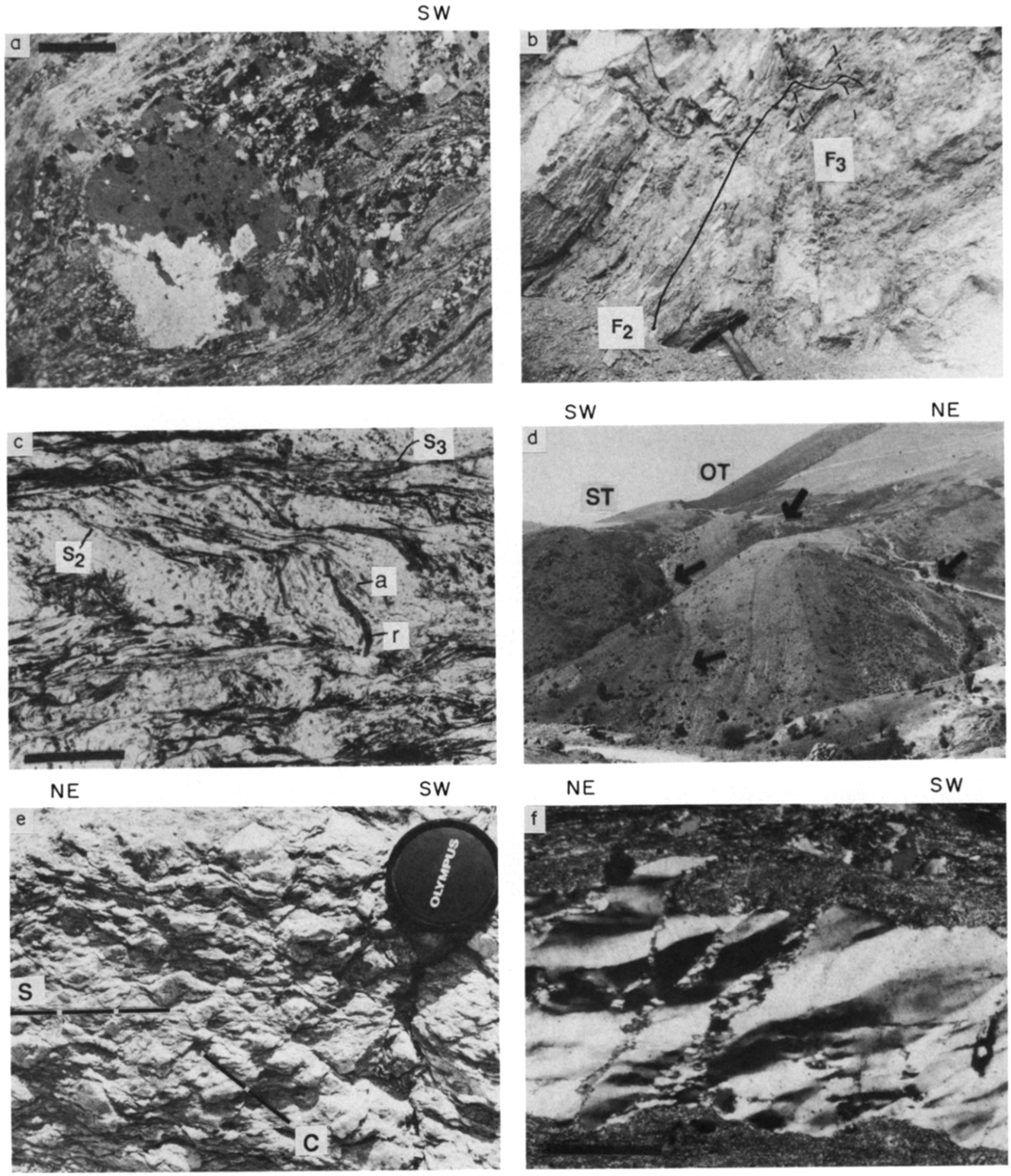

Fig. 7. Photographs of structures developed during D_1–D_3. (a) Photomicrograph of coarse K-feldspar augen in a mylonite from adjacent to the D_1 thrust on Trohalos ridge (Fig. 1), showing dynamic recrystallization of feldspar. Center of grain shows grain-boundary migration recrystallization and subgrains while edges are surrounded by very fine-grained neoblasts. Crossed nicols, scale bar 1 mm. Similar textures are seen in K-feldspars in mylonites adjacent to D_2 thrusts. (b) F_2 and F_3 folds fold alternating granitic–amphibolitic layers (S_1) in Infrapierien (Livadi) gneiss. F_2 axial trace shown by solid line, F_3 shown by dashed lines. Hammer handle is 30 cm long. (c) Photomicrograph of S_2 fabric in Pierien unit defined by phengite + riebeckite + acmite folded about F_3 folds; S_3 axial-planar cleavage contains the same mineral assemblage. Riebeckite = r; acmite = a. Plane light, scale bar 1 mm. (d) View of Olympos (OT, arrows) and Sparmou (ST, arrows) thrusts from the southern margin of Olympos window, near Monastery Sparmou. View toward the northwest; thrusts dip to the southwest. In this area the Olympos thrust is located in a strongly mylonitic zone between flysch of the Olympos unit and calcareous graywacke of the Ambelakia unit (overlain by the marble which forms the ridge in the center of the photograph). Limestone of the Olympos unit forms the light grey hillslope in the upper right corner. The Sparmou thrust is defined by the contact between mylonitic gneiss of the Pierien unit above (dark rocks on left), and marble of the Ambelakia unit below. (e & f) Sense of shear indicators along the Sparmou thrust. Southwest is to the right; sense of shear is top-to-the-southwest. Outcrop view (e) shows asymmetric augen and *S*–*C* fabric; photomicrograph (f) shows inclined deformation bands in a quartz ribbon. *C* planes defined by phengite are parallel to the long dimension of the photograph. Crossed polars, scale bar 1 mm.

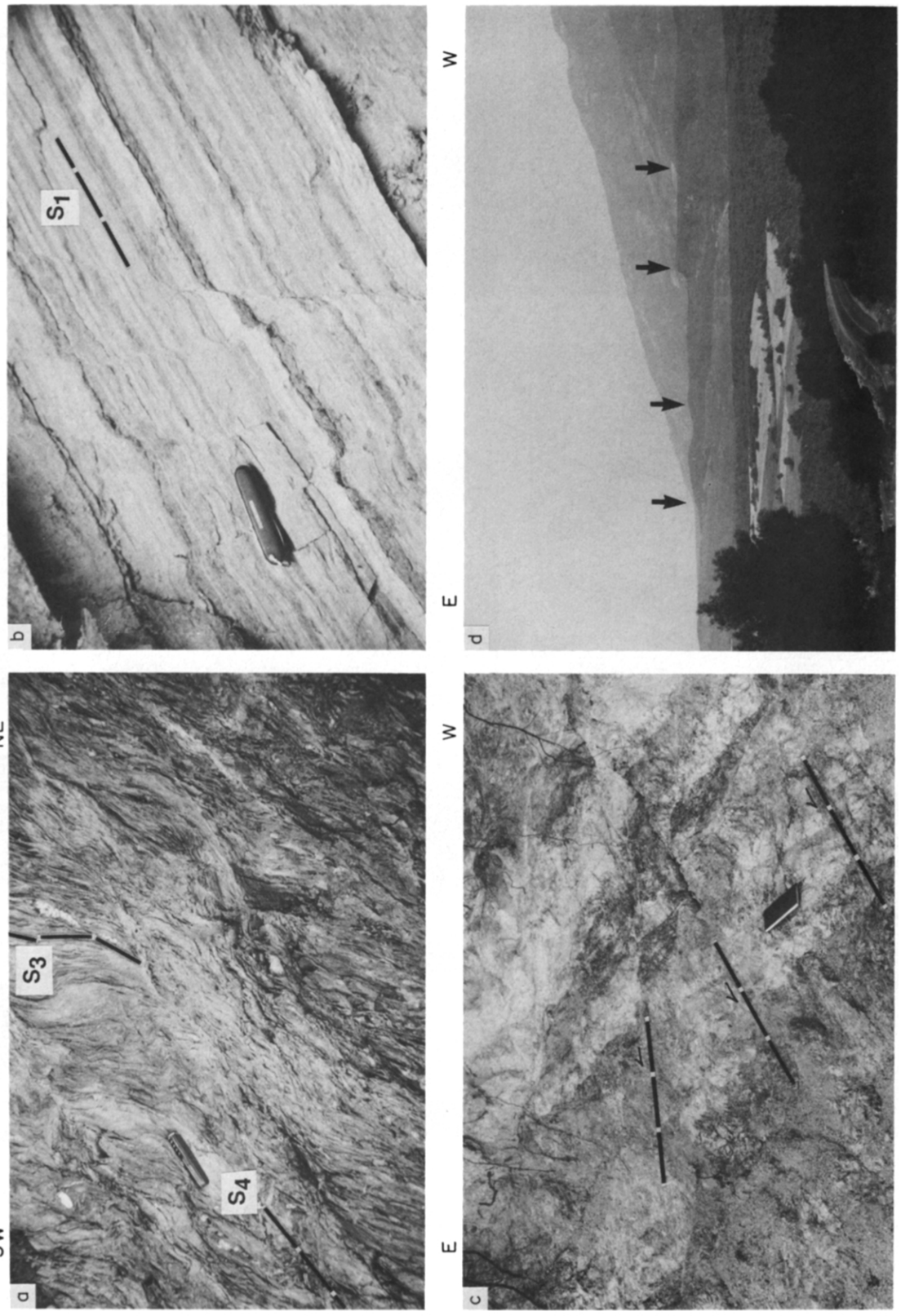

Fig. 8. Photographs of deformation features related to D_4–D_7. (a) Mesoscopic shear fabric in Ambelakia unit metagraywackes from the southwest margin of the Olympos window, showing top-to-the-northeast sense of shear. Note that S_3, the mylonitic fabric associated with the Olympos thrust, is cut by the S_4 shear planes, indicating that the NE-vergence is not related to movement along the Olympos thrust. (b) Semi-ductile normal faults cut S_1 fabric in Infrapierien gneiss, north flank Mt. Olympos. Such small-scale normal faults may be related to D_5 low-angle normal faults that crop out <1 km to the south. (c) Brecciated limestone and dolomite of the Olympos unit on the eastern flank of Olympos near Litochoro village (location in Fig. 1). Carbonate rocks form the footwall to a high-angle normal fault (D_7) with serpentinite melange in the hanging wall. Note abundant normal-sense offsets of limestone and dolomite layers. (d) View to the south from northern margin of Mt. Olympos along young normal fault scarps that cut Neogene and Quaternary conglomerate in the basin northeast and east of the mountain range. Four scarps can be seen in this photograph (arrows). The gentle slope in the background is a dip-slope of Olympos unit Triassic dolomite and limestone in the east limb of a broad fold.

tures are attributed to D_2 because they apparently do not affect the Olympos unit (Figs. 1 and 2b; Fig. 3, locations 1 and 3; Fig. 5, C–C′). Gneiss, schist and marble contain a NE-trending mineral lineation parallel to the axes of tight-to-isoclinal F_2 folds; S_2 axial-planar foliation is variably developed and folded by microscopic to mesoscopic close to isoclinal F_3 folds (e.g. Fig. 7b). Near Karfia Ridge (Fig. 1), NW-verging tight to isoclinal folds with meter to tens of meters wavelengths involve the Ziliana, Ambelakia and Olympos units together and thus are interpreted as F_3 (Fig. 4, location 1; Fig. 5, D–D′).

Pierien unit

The Pierien unit exhibits well-developed D_2 microstructures along the Sparmou thrust, but the lithologically homogeneous nature of the unit precludes recognition of large-scale structures except where marbles are involved. A strong mylonitic fabric is present in the granitic gneisses and mica schists along the western flank of Mt. Olympos (Figs. 1, 3 and 7e & f). The S_0/S_1 compositional layering in Pierien gneiss and marble is transposed into parallelism with the Sparmou thrust (Fig. 3, location 5). The SW-plunging mineral lineation defined by sodic amphibole and pyroxene is parallel to the stretching lineation defined by elongate quartz and feldspar grains and also subparallel to the fold axes of (F_3) isoclinal microfolds that fold the S_2 fabric (Fig. 7c). Although the entire Pierien thrust sheet was not examined in this study, a transect through higher portions of the thrust sheet south of Mt. Olympos revealed the presence of similar SW-plunging lineations and thin mylonite zones more than 3 km structurally above the Sparmou thrust, suggesting that the Pierien unit in this area may be internally imbricated (although the relative age of the shear zones is uncertain).

Ambelakia unit

In the Ambelakia unit a greenschist to blueschist–greenschist transition facies metamorphic foliation occurs as mesoscopic to microscopic floating fold hinges within the marbles and schists. The foliation is overprinted by S_2 and associated blueschist facies minerals, but it is unclear whether the earlier fabric is part of D_2 or a distinct event, D_1, that might have affected only part of the Ambelakia unit (Table 1).

The S_0 (S_1?) fabric, outlined by cherty, dolomitic, and phyllitic layers in the marbles, and by the marble–schist compositional layering, is isoclinally folded about axes that trend NE and are attributed to F_2 where they are associated with the Sparmou thrust or affect only the Ambelakia unit (Fig. 2a; Fig. 4, location 2; Fig. 6). The lineation, defined by mineral elongation in the schists and a calcite shape fabric in the marbles, is subparallel to fold axes (Fig. 6).

F_3 folds in the Ambelakia metasediments typically have NE-trending axes (Fig. 6) and extremely thinned limbs; S_3 is well developed (Fig. 8a). Clasts within local pebbly layers in the calcareous rocks exhibit a strong flattening perpendicular to the S_3 foliation and elongation parallel to the mineral lineation. Interference of F_2 and F_3 isoclines forms type 3 (Ramsay 1967, p.530) interference patterns.

Olympos unit

D_3 is the first event to affect the Olympos unit, where it is expressed as a well developed S_3 cleavage associated with a variety of fold styles (Table 1). The cleavage is axial planar to isoclinal folds locally visible in thin section and outcrop as refolded or floating hinges. S_3 is also folded by small-scale tight to isoclinal folds that typically plunge northeast or southwest and have steeply NW-dipping axial planes. Mesoscopic folds occur as parasitic folds to the map-scale overturned syncline in the flysch northeast of Kokkinopilos (Figs. 1 and 2b; Fig. 3, location 6; Fig. 5, C–C′). Locally, F_3 folds are cut by the Olympos thrust, but the thrust is also folded by tight subparallel folds interpreted as late-stage F_3 (Fig. 3, location 7; Fig. 4, location 1; Fig. 5, C–C′, D–D′). Although D_3 includes pre-thrust folds, syn-thrust folds and post-thrust folds, the timing relative to earlier (D_2) and later (D_4) events is the same, and the kinematics of folding and faulting is apparently the same (see below). Thus I interpret the folds and the Olympos thrust to be D_3 structures. D_3 is easily distinguished from D_4 by orientation, style (Table 1) and penetrative axial-planar foliation.

The Sparmou thrust

The D_2 fault between the Pierien and Ambelakia units is exposed along the western to southern flanks of Mt. Olympos. This thrust fault is here named the Sparmou thrust after the excellent exposures near Monastery Sparmou (Figs. 1, 2 and 7d). The Sparmou thrust is marked by a well-developed mylonite zone that ranges in thickness from ~50 to 300 m, but strongly sheared rocks are present in thin parallel bands up to 1000 m above the thrust. Structures formed by non-coaxial shear parallel to the well-developed mylonitic lineation are present in outcrop and thin sections (Figs. 7e & f). In the Kokkinopilos area, the thrust occurs as a zone of steeply W-dipping imbricate faults (Fig. 3, location 8; Fig. 5, A–A′). Isoclinal folds are both cut by and fold the Sparmou thrust in several locations (e.g. east of Sparmou, Fig. 2a; Fig. 3, location 4); S_1 is pervasively transposed into S_2 and the underlying Olympos unit is unaffected, suggesting the folds are F_2.

The Olympos thrust

The D_3 Olympos thrust is defined by the well-developed mylonite zone which separates the Olympos unit from the Ambelakia unit. It is commonly difficult to distinguish the Ambelakia unit from the Olympos unit in the thrust zone, however, the contact typically occurs between Olympos unit metaclastic rocks (flysch) and Ambelakia unit cherty and/or platy marbles, so in the absence of a visible mylonite zone, the thrust is mapped along this contact. However, in many areas the thrust is located where the strongest mylonitic fabric occurs within a zone of metaclastic rocks or between two

marble horizons (e.g. Fig. 3, location 9; Fig. 7d). West of Kallipevki the Olympos thrust cuts out the Ambelakia unit and the Sparmou thrust, juxtaposing the Olympos and Pierien units (Figs. 1, 2b, 4 and 5, B–B′).

Well developed *L–S* mylonites occur along the Olympos thrust. In the Ambelakia unit of the hanging wall, the S_3 mylonitic foliation is parallel to the axial planes of refolded F_2 isoclinal folds and the stretching lineation trends NE, parallel to a crossite mineral lineation. For >800 m structurally below the thrust, a stretching lineation formed by quartz and feldspar in the flysch and by a calcite shape fabric in the limestones is oriented ~N50E, sub-parallel to the fold axes (Figs. 3 and 6). The thin sliver of mylonitic flysch along the western to the southern margin of the window contains asymmetric augen and pressure shadows; locally *S–C* fabrics are developed. There is strong flattening perpendicular to the schistosity and elongation parallel to the inferred transport direction.

Ophiolite unit. Variably-oriented tight to isoclinal folds that fold the S_1 foliation and contain a well-developed axial-planar cleavage occur in greenschist facies calcareous schist and marble enclosed within the serpentinite–matrix melange of Lizadiko ridge (Table 1, Figs. 1 and 9, unit Mzm1). The folds have wavelengths from a few centimeters to several meters and are discordant to the foliation and folds in the surrounding ultramafic rocks. Igneous rocks of the ophiolite unit are typically foliated, but the intensity of fabric development and the orientation of the foliation vary widely over short distances, so it is difficult to determine the large-scale geometry of this deformation. Gabbroic and basaltic rocks locally contain two foliations interpreted as S_1 and S_2; both foliations apparently formed under greenschist facies conditions. The second foliation is axial planar to tight folds.

The variable orientation and lack of blueschist facies metamorphism in post-D_1 structures in the ophiolite unit make it difficult to correlate these structures with D_2/D_3 or younger structures in adjacent units. The structures are tentatively assigned a D_2 relative age, but it is possible that the deformation occurred while the ophiolite unit was widely separated from the nappes of the Olympos region and is unrelated to D_2 in the continental units.

D_2 *and* D_3 *kinematics.* The mylonites along the Sparmou and Olympos thrusts contain variably developed shear-sense indicators, including *S–C* fabrics, asymmetric feldspar augen and pressure shadows, and oblique elongate recrystallized quartz grains and subgrains (Figs. 7e & f). Because the Ambelakia unit is so thin and mylonitic throughout, it is difficult to distinguish D_3 from D_2 shear fabrics. Outcrops of mylonitic Olympos flysch are generally poor and commonly have variable attitudes due to small-scale folding, thus only a few oriented samples were suitable for kinematic analysis.

The majority of samples of the Pierien and Ambelakia units show a SW-directed sense of shear (Fig. 6), although many samples contained ambiguous evidence for the shear direction (either no indicators or both up- and down-plunge senses, shown as double-headed arrows in Fig. 6). The variation in trend from S30W to S70W is the result of later folding. Several samples were cut perpendicular to the lineation (*y–z* sections) in order to confirm that the displacement direction was parallel to the lineation. In all cases, no dominant shear sense could be determined from the *y–z* sections. This observation suggests that the NE-trending isoclinal folds do not reflect transport of thrust sheets perpendicular to the fold axes, as interpreted by Schmitt (1983), but instead reflect either rotation of the fold axes into the transport direction or initiation of the folds in this direction (e.g. Escher & Watterson 1974).

Independent data for the shear direction along the D_3 Olympos thrust, while sparse, come from the Olympos flysch and the base of the Ambelakia unit (Fig. 6a), and support the SW-vergence interpreted for the Sparmou thrust. Geometric and stratigraphic arguments provide additional support for SW-vergence of the Olympos thrust: the Sparmou thrust and the Olympos thrust are sub-parallel, and D_2 and D_3 lineations and isoclinal fold axes are parallel (Figs. 6d & f). The Olympos thrust is always in a lower structural position, and movement along it must post-date movement along the Sparmou thrust. This geometry suggests that the Sparmou thrust was carried 'piggy-back' in the hanging wall of the Olympos thrust. In the study area, the Olympos thrust always contains the Olympos unit in the footwall and either the Ambelakia or Pierien unit immediately above the thrust; if the Sparmou thrust were SW-directed and the Olympos thrust were NE-directed, the Ambelakia unit should overthrust the Pierien unit, and this is not observed. The Olympos thrust ramps up from Triassic rocks in the eastern portion of the window to Cretaceous and Tertiary rocks on the western margin (Fig. 1) (Schermer 1989, 1990, Vergély & Mercier 1990), consistent with the observation that thrust faults ramp up (not down) in the direction of transport (Royse *et al.* 1975).

Microfolds in carbonates and flysch of the Olympos unit studied by Vergély & Mercier (1990) are also interpreted to reflect SW vergence of the first deformation experienced by this unit and associated movement along the Olympos thrust.

Metamorphic and microstructural evidence for P–T conditions. Blueschist facies mineral assemblages are widely developed throughout the Pierien and Ambelakia units at Mt. Olympos. M_2 conditions have been estimated at $T < 350$°C, $P \sim 5$–8 kb; M_3 temperatures were likely somewhat lower (<250°C; Godfriaux *et al.* 1988, Schermer 1990). S_2 mylonites are associated with blueschist facies mineral assemblages in Pierien and Ambelakia units adjacent to the Sparmou thrust and at higher structural levels in the Pierien nappe (Fig. 7c). Sodic amphibole and pyroxene form mineral lineations parallel to the stretching lineation, suggesting contemporaneous metamorphism and deformation. Blueschist

facies minerals occur parallel to S_2 and S_3 in the Ambelakia unit. The Olympos unit, although not strongly recrystallized, contains crossite, lawsonite and phengite parallel to S_3 in the Olympos flysch (Schermer 1990). The metamorphic evidence is consistent with Ar/Ar data which show that D_1 and older white micas were not reset during later events, suggesting temperatures remained below 350°C. Calcite–dolomite geothermometry in Olympos unit limestones adjacent to the thrust suggest $T \sim 400$°C and an inverted thermal gradient that is interpreted to be the result of shear heating along the thrust (Barton & England 1979).

Deformation mechanisms in mylonites along the Sparmou and Olympos thrusts, however, suggest higher temperatures for the mylonitization. Quartz exhibits various degrees of dynamic recrystallization, including undulatory extinction, incipient and well-developed subgrains, ribbons and aggregates of neoblasts (Fig. 7f). Domains of strongly oriented crystallographic fabric in quartz are observed. Feldspars are commonly broken and cracked; however, in some samples, subgrains occur within the augen, and dynamically recrystallized grains occur along the perimeter of the augen, indicating ductile behavior in feldspars during mylonitization. These deformation mechanisms suggest temperatures approaching 450°C (Simpson & De Paor 1991), 100–200°C higher than that inferred from the metamorphic assemblages. Possible reasons for this discrepancy will be discussed below.

D_2 *and* D_3 *timing.*

Continental units

Constraints provided by stratigraphic and radiometric data suggest that D_2 and D_3 were the result of two distinct events that occurred under similar *P–T* conditions. Ar/Ar ages suggest the D_2 Sparmou thrust is early Eocene (>53 Ma, Table 1), although blueschist metamorphism and deformation may have begun during Paleocene time (~61 Ma). The presence of Lutetian fossils in the Olympos flysch (Godfriaux 1968) indicates that D_3 must be younger than 50–42 Ma (Harland *et al.* 1990), and Ar/Ar data suggest it is 36–42 Ma. It is possible that D_2 and D_3 represent a broadly continuous period of deformation from ~60 to 40 Ma.

Ophiolite unit

The principal difference between possible D_2 structures in the ophiolite unit and those affecting other units is that the former were clearly *not* formed under blueschist facies conditions. Because the geometric and kinematic characteristics of D_2 structures in the ophiolite unit have been obscured by later melange formation (D_5?), it is impossible to correlate the structures. The deformation and greenschist facies metamorphism affects Maestrichtian(?) carbonate rocks that appear to locally depositionally overlie the ophiolite (Godfriaux & Pichon 1980), thus the metamorphism and associated structures described above as D_2 must have occurred in latest Cretaceous or Tertiary time. The absolute age is unknown, however, and it is uncertain whether this deformation event in the ophiolite unit is regionally correlative with D_2 or younger events.

D_4: *NW–SE folding*

D_4 is manifested by map scale and outcrop scale NW-trending folds (Figs. 2b and 6; Fig. 4, locations 5, and 6) that reflect continued shortening following D_2 and D_3 thrusting. In addition to its distinct orientation, D_4 is distinguished from earlier events by its typically weak penetrative fabric and lack of metamorphism, although prehnite–pumpellyite facies assemblages may be late-to post-kinematic with respect to D_4 (Schermer 1990).

D_4 folds are best developed along the southwestern to western margin of the Olympos window, where the Sparmou and Olympos thrusts are folded into an upright antiform–synform pair (Figs. 1, 2b and 4; Fig. 5, B–B′). Locally, the F_4 folds are associated with a spaced cleavage that is best developed in calcareous schists and sandstones of the Ambelakia unit and the flysch of the Olympos unit (Fig. 8a). The intersection of S_4 and S_3 and shear on the limbs of F_4 folds produces a NE-vergent mesoscopic shear fabric on the southwest limb of the fold west of Karia (Fig. 8a). The trends of F_4 folds vary from ~N75W to N40W, with moderate plunge to both northwest and southeast (Figs. 2b and 6). Bedding within the Olympos window also appears to have been folded about F_4; the distribution of F_3 and L_3 suggests the F_4 axis is oriented ~N45W (Fig. 6).

D_4 *kinematics,* P–T *conditions and timing.* Small-scale F_4 folds verge both northeast and southwest (Fig. 3; Fig. 4, east of location 5). Map-scale F_4 folds are typically not strongly asymmetric. On the southwestern margin of the Olympos window, however, the map-scale folds are NE vergent; these folds may be parasitic folds on the southwest limb of a broad antiform whose east limb has been faulted out along the eastern margin of the Olympos window (see D_7), and thus would reflect the expected sense of shear for that limb (e.g. Fig. 4, location 3; Fig. 5, B–B′; Fig. 6a). Because the folds are relatively open, they probably do not represent folds parallel to transport direction as do F_2 and F_3, but are perpendicular to late stages of the NE–SW shortening that was responsible for D_2 and D_3. The lack of associated metamorphism and less-penetrative nature of D_4 structures indicates that deformation occurred at a shallower level and at lower temperatures than D_2 and D_3. The broad F_4 fold that affects the Olympos window and surrounding rocks (Fig. 2b) may be interpreted as a ramp anticline on a thrust below the Olympos unit. The presence of a lower thrust is consistent with evidence for contemporaneous thrusting in the external Hellenides if these thrusts are rooted beneath the Olympos unit (e.g. Bernoulli & Laubscher 1972, Jacobshagen *et al.* 1978).

F_4 folds were interpreted by Barton (1976) to indicate

NE-vergent thrusting of the Flambouron unit over the Olympos unit. Using the Hansen (1966) technique to analyze folds within the Olympos unit as well as in the overthrust gneisses in the Sparmou area, Barton determined that the gneisses were transported towards ~N45E above the Olympos thrust. The data presented herein indicate that both large- and small-scale NW-trending folds fold the mylonitic fabric in hanging wall and footwall of the Olympos thrust and that map-scale folds fold the thrust. Thus the northeast transport direction determined by Barton (1976) is associated with post-thrusting (i.e. D_4) shortening rather than with movement along the Olympos thrust (i.e. D_3). Similar conclusions were reached by Vergély & Mercier (1990).

The double plunge of the F_4 map-scale folds in Karia and Kallipevki areas suggests that they are refolded about younger (F_6) axes (Fig. 2b; Fig. 4, location 6). Ar/Ar data do not directly date D_4, but constrain it to be post-36 Ma and pre-16–23 Ma (Table 1).

D_5: *low-angle normal faults*

Brittle low-angle faults formed during D_5 cut D_1–D_4 structures and juxtaposed rocks of the ophiolite unit against all structurally lower nappes. The cross-cutting relationship between D_5 faults and older thrusts is best observed at the southwest end of Lizadiko ridge (Figs. 1 and 9). Southwest of the intersection of the Lizadiko Ridge and Keri Ridge faults with the Olympos and Sparmou thrusts, the entire thrust succession is intact, from the Olympos unit to the Infrapierien and ophiolite unit (Livadi complex), whereas to the northeast, the fault below the ophiolite and Infrapierien (Paleambela) units cuts across the entire thrust stack. Gouge or fault breccia is commonly present along the faults and cataclastic fabrics overprint earlier ductile (mylonitic) features (Fig. 8b). Cataclastic and semi-ductile shear fabrics are present in the footwalls up to a few meters below the fault surfaces and hanging wall rocks are

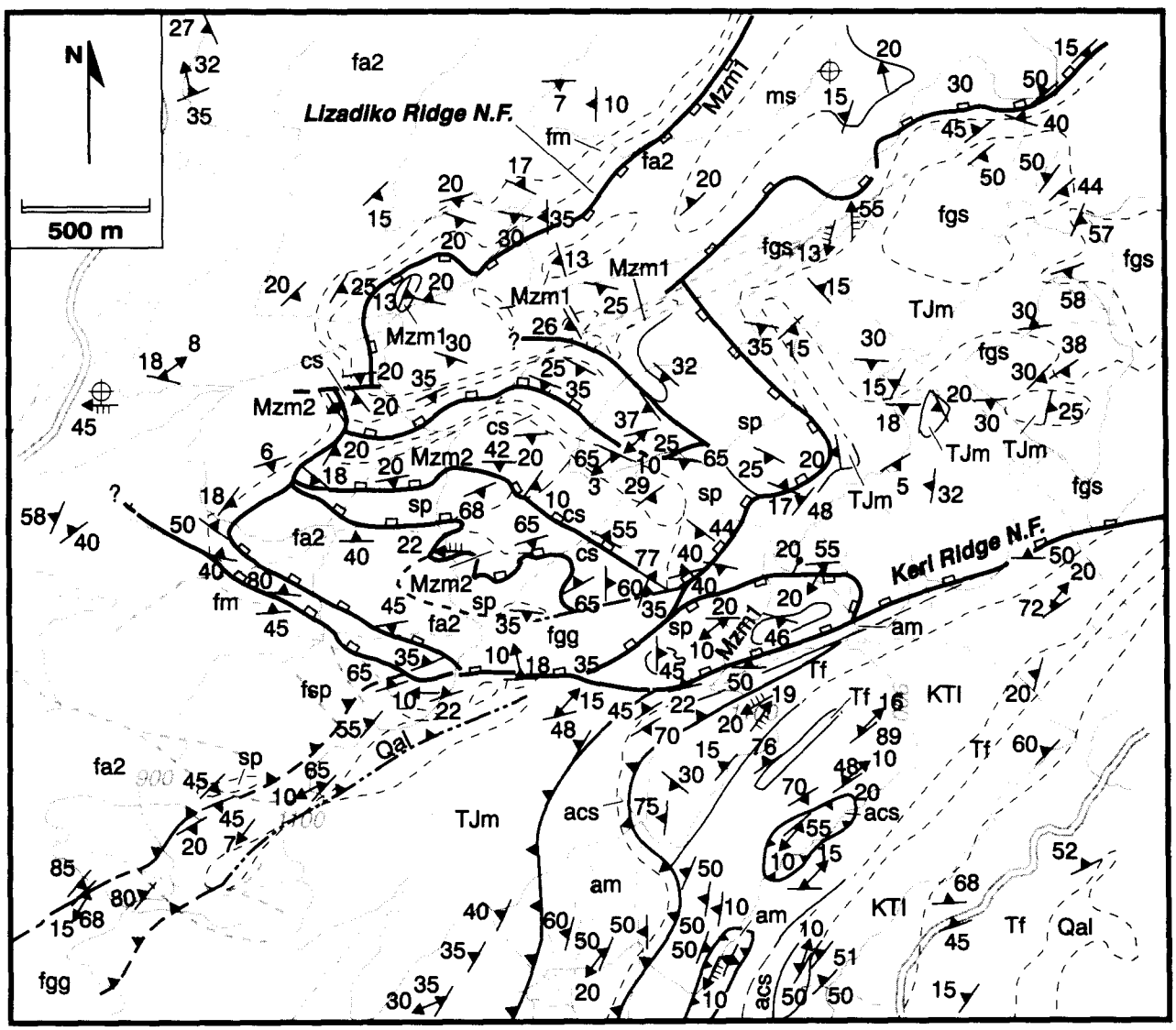

Fig. 9. Map of the west end of Lizadiko ridge, with location shown in Fig. 1; map symbols as defined in Fig. 5. Lizadiko ridge normal fault system and imbricate normal faults in its upper plate are shown in bold lines. Note that the sequence sp–cs–Mzm2 (serpentinite–calcareous schist–marble) dips SSW and is repeated by NNE-dipping normal faults that do not cut the basal low-angle fault except in one location, where the offset is minor.

intensely faulted. Locally (e.g. the west end of Lizadiko ridge), where the ophiolite unit forms the hanging wall, the rocks are mixed in a thick (>250 m) zone of serpentinite–matrix melange (Fig. 9). The Kallipevki fault cuts F_4 folds (Fig. 4, location 3); D_5 faults on the northern flank of Mt. Olympos neither cut nor are folded by F_4.

The major D_5 faults appear to have a listric geometry. The southern parts of the Lizadiko Ridge and Keri Ridge faults are fairly high-angle (~60°C), yet the faults curve to low angles toward the northern segments (Figs. 2c and 9). It is unlikely that the apparent listric geometry is the result of two fault systems (an early low-angle one and a later high-angle one) because rocks in the footwalls of the low-angle faults are not cut by major high-angle faults (Figs. 1 and 9). The Kallipevki fault is 'scoop'-shaped, opening in a northeastward direction (Fig. 4; Fig. 5, D–D′). High-angle normal faults with a total of ~500 m of down-to-the-northeast vertical displacement offset the Kallipevki fault (Fig. 2c; Fig. 4, location 4; Fig. 5, B–B′).

D_5 *kinematics*. Although all low-angle faults were interpreted by previous workers as thrust faults (Godfriaux 1968, Schmitt 1983, Migiros 1985, Vergély & Mercier 1990), I interpret the Lizadiko Ridge and Keri Ridge faults and the Kallipevki fault system (Figs. 1, 4 and 9) to be normal faults based on the following evidence. (1) The map pattern of the faults indicates that they are discordant to the earlier thrust-related structural succession and consistently place the highest structural levels against the lowest structural levels on faults which omit section. (2) The low-angle faults are not associated with folds as are typically observed adjacent to the D_1–D_3 thrust faults. (3) Local kinematic indicators such as semi-ductile shear fabrics, drag folds and small-scale faults associated with the major faults (Fig. 8b) suggest normal-sense displacement. Although Vergély & Mercier (1990) have proposed a period of 'opening' of the window by erosion, followed by thrusting, to explain the missing structural section between the ophiolite unit and underlying units, they present neither stratigraphic and sedimentologic evidence for such erosion nor structural evidence for the sense of movement along the young low-angle faults.

Direct kinematic evidence from D_5 fault surfaces has not been found due to poor exposure. In the Lizadiko Ridge area, south-southwest tilting of fault blocks in the hanging wall suggests displacement of the hanging wall to the north-northeast (Fig. 9). The NW orientation of the ramp in the Keri Ridge normal fault (Fig. 5, A–A′) also is consistent with a northeast displacement direction, although it is possible that the entire normal fault system has been rotated during later deformation. Sparse semi-ductile shear fabrics observed in thin sections from the low-angle segment of the Kallipevki fault suggest top-to-the-northeast (normal) sense of shear (Fig. 6a, open arrows).

D_5 *timing*. In addition to the cross-cutting relationships described above, constraints on the relative age of the D_5 faults at the base of the ophiolite are provided by the metamorphic history. The ophiolite unit contains only greenschist facies rocks, whereas the footwall units contain blueschist facies rocks. Ar/Ar data suggest the age of the blueschist metamorphism (D_2–D_3) is latest Cretaceous to middle Eocene, yet the age of ophiolite obduction is considered by most workers (Mercier *et al.* 1975, Vergély 1976, Katsikatsos *et al.* 1982, Schmitt 1983) to be latest Jurassic to Early Cretaceous. If the ophiolite had been emplaced by thrust faulting prior to Eocene time, it should contain evidence of blueschist facies metamorphism. The absence of this metamorphic event supports the interpretation that the emplacement of the ophiolite in the Mt. Olympos region was the result of post-D_3 deformation.

The melange structure within the ophiolite unit on Lizadiko ridge is of uncertain age; the foliation in the serpentine is variably oriented (Fig. 9); it is locally parallel to the boundaries of individual marble blocks within the melange, but has no relation to the folds within the marble and schist blocks. Thus the melange structure must post-date D_1 and D_2 folding and metamorphism, yet is apparently unaffected by D_3 and D_4, and thus is tentatively assigned to D_5.

Ar/Ar data on potassium feldspar from samples below the low-angle segment of the Kallipevki normal fault indicate cooling of the metamorphic rocks below ~150°C began in early to middle Miocene time (~16–23 Ma). Schermer *et al.* (1990) interpret this cooling to indicate movement of the metamorphic rocks toward the surface and to be related to the beginning of extension.

D_6: *NE–SW open folds*

The youngest folds are attributed to D_6. These include open, symmetric and upright ~N40E-trending folds that affect all units (Fig. 2c). F_6 folds are particularly well exposed on the east side of Karfia ridge south of Kallipevki village (Fig. 1; Fig. 4 east of location 5; Fig. 5, D–D′). In this region, the complicated outcrop pattern is the result of the superposition of F_2, F_3, F_4 and F_6 folds. The NE-trending elongate windows and klippen of Olympos flysch and Ambelakia marble are the result of F_2 and F_3 isoclinal folds; close to open F_4 and F_6 folds produce an elongate dome-and-basin pattern of the interfolded Olympos and Ambelakia rocks. The symmetric, upright F_6 folds plunge ~S40W and have a wavelength of 1–2.5 km. Folds of the same style and similar orientation but longer wavelength (4–5 km) affect the F_4 folds west of Kallipevki (Fig. 4, location 6) and near Karia, and may also be partly responsible for the domal structure of the Olympos window (Fig. 2c). Northeast-plunging open, upright folds in the Paleambela nappe and Keri Ridge normal fault are attributed to F_6 (Fig. 2c) due to the similarity of style, orientation and lack of cleavage.

D_6 *kinematics and timing*. The kinematic significance of D_6 structures is enigmatic. If F_6 folds are related to shortening, the shortening direction would be perpendicular (NW–SE as opposed to NE–SW) to that recorded by D_1–D_4. The difference in wavelength and tightness of the D_6 structures within the allochthonous rocks and the carbonate massif of the Olympos window may be due to the greater layer thickness and competence of the carbonate rocks relative to the flysch and thin thrust sheets of marble, schist and gneiss.

While there are no tight absolute age constraints on the timing of D_6, it is bracketed by the age of F_3 structures which are folded (36–40 Ma, Table 1), and Neogene conglomerates which are not folded. The effect of D_6 structures on F_4 folds in the southern Olympos region constrains the relative timing of these fold phases. The relationship between D_5 and D_6, however, is not as clear. The location of the structurally highest unit (the ophiolite) at topographically low positions north-northwest and south-southwest of 3-km high rocks within the Olympos window and the interpretation of the Lizadiko ridge and Kallipevki faults as low-angle normal faults suggests that if these normal faults were once part of the same system, they may have been warped about F_6 axes (Fig. 2c). The broadly similar geometries and apparent displacement directions may be indicative of the once contiguous nature of these two fault systems. The interpretation that D_5 normal faults are warped about F_6 folds cannot be proven because the D_5 faults cannot be traced around the margin of the Olympos window. F_6 folds in the Paleambela area are cut by the Keri Ridge normal fault (Fig. 2c), thus at least some movement on the Keri Ridge normal fault postdates the formation of these folds and it is possible that D_5 and D_6 are broadly coeval.

The timing and apparently dissimilar kinematics of D_6 folds suggest that the broad domal structure of the window and the doubly-plunging F_4 folds may not be the result of cross-folding, but instead are large-scale corrugations of D_5 low-angle normal faults and/or related to drag and uplift of the crust in the footwall of D_5 and D_7 normal faults. Similar corrugations have been noted by workers in other areas of Greece (Dinter 1991) and in metamorphic core complexes of the U.S. Basin and Range province (e.g. John 1987).

D_7: *high-angle normal faults*

The final phase of deformation consists of high-angle NE- and E-dipping normal faults. These faults juxtapose ophiolitic rocks against Triassic limestone of the Olympos unit on the eastern margin of the window (Figs. 1 and 2c; Fig. 5, A–A′). In contrast to the D_5 low-angle normal faults, brittle deformation related to D_7 normal faults extends well into the footwall rocks (>100 m locally), and both hanging wall and footwall rocks are intensely brecciated (Fig. 8c). Locally, gouge zones are >10 m thick. Fault scarps within Neogene and Quaternary conglomerates occur along the northern flank of Mt. Olympos (Figs. 1, 5 and 8d); the dips of 60° indicated for these faults on section A–A′ are probably minima because the dips are measured on the fault scarps which have been eroded. In general there are no marker beds in the hanging walls and footwalls to constrain the amount of offset, but the scarps pictured in Fig. 8(d) range from 5 to 15 m high. Conglomerate in the hanging wall is locally tilted as much as 25°; variable backrotation of hanging wall units may suggest the D_7 faults are listric. Reconnaissance investigations indicate that similar faults occur on the eastern flank of the Pieria mountains to the north. D_7 faults appear to be part of an important network of very young (and locally active) high-angle normal faults that bound the eastern flank of the mountains from the Yugoslavia border, along the western margin of the Vardar basin, to southeast of the Olympos region, where they strike offshore and form the western boundary of the north Aegean.

D_7 *kinematics*. None of the D_7 faults examined in this study contained visible polished surfaces or slickenside lineations, so it is difficult to determine the displacement direction. Small-scale faults in the breccia zone along the eastern flank of Mt. Olympos (Fig. 8c) have a down-to-the-east dip-slip component. The geometry of offset units in cross-section requires some down-dip component of displacement. Schmitt (1983) however, characterized many of the high-angle faults in the Olympos region as strike-slip faults. Many of the strike-slip faults shown on her map must have some component of normal displacement as they juxtapose units from different structural levels even where the units are horizontal. I could not confirm the presence of a major strike-slip faulting event on the basis of either map-scale structures or minor folds and shear zones.

The tectonostratigraphic throw on the normal faults along the eastern flank of Mt. Olympos, a cumulative displacement on D_5 and D_7 faults, may be as much as 6–8 km, the approximate thickness of the excised thrust sheets. It is important to note, however, that if these blueschist facies rocks were once at >20 km depth (Schermer 1990), a good deal more cover has been removed than is evident here (see below).

D_7 *timing*. D_7 faults cut D_5 faults (Fig. 2c). The high-angle faults attributed to D_7 are not folded by F_6 and thus must be younger. The conglomerates and marls designated as Quaternary and Neogene are not precisely dated, however, the fact that scarps remain visible on these faults even in the relatively poorly consolidated marly rocks indicates they may be recently active faults.

DISCUSSION

Structural characteristics of intracontinental subduction

D_1–D_4 deformation involved large-scale shortening and high pressure–low temperature metamorphism of the continental basement of the Pelagonian zone and its carbonate cover. Deformation progressed toward the

foreland (southwestward) and to lower structural levels with time. Units at high structural levels were only weakly deformed during later events (e.g. weakly developed D_2–D_3 in Infrapierien nappes) and are interpreted to have been carried 'piggyback' above lower thrusts. Within each major thrusting event there is an evolution of structures related to overall progressive simple shear, from (1) the formation of syn-metamorphic isoclinal folds and axial-planar schistosity to (2) thrusting associated with the formation of mylonitic foliation and stretching lineation to (3) folding of the thrust. Each of these stages appears to record not only the same sense of shear, but also a similar NE–SW orientation, suggesting that early-formed structures probably have been rotated into parallelism during progressive strain. An estimate of minimum shortening during D_1–D_4 is provided by restoring the major thrusts across the Olympos window; the overlap requires >70 km shortening (~75%) without restoring small-scale folds or ductile strain.

Thrust sheets of the Paleozoic basement rock are thin (~250 m locally), and must have been detached from the lower crust. That upper parts of the basement were underthrust to depths >20 km and metamorphosed at high pressure–low temperature conditions suggests that continental crust was subducted. The exposed basement nappes were decompressed during thrusting above carbonate rocks of the Olympos and lower units (D_3–D_4), and exhumed by the removal of tectonic overburden by D_5–D_7 normal faulting and erosion. Because the lower crustal portions of the Flambouron nappes are not exposed, and the crust here is only moderately thick (45–50 km; Makris 1977, Giese *et al.* 1982), the lower parts of the continental crust may have been subducted into the mantle. Although it is generally assumed that continental crust is too buoyant to be subducted into the asthenosphere, calculations by Molnar & Gray (1979) indicate that if the upper crust is detached from the lower crust, and if the continent is attached to subducting oceanic lithosphere, the gravitational body forces are sufficient to cause subduction of tens to hundreds of kilometers of the continental crust. Thus the estimate of >70 km shortening and ≥20 km depth reached by parts of the Pelagonian crust is not unreasonable. In many collisional orogens, several hundred kilometers of crustal shortening are inferred from geologic relations and require subduction of significant amounts of lower crust (e.g. Bally 1975, Burchfiel 1980, Hodges *et al.* 1982).

Shortening began during middle Cretaceous time and continued until after middle Eocene time. Some workers (e.g. Mercier 1968) interpret stratigraphic, structural and metamorphic evidence for ophiolite obduction and deformation in latest Jurassic–Early Cretaceous time to suggest that the Vardar ocean closed before Late Cretaceous time. Others (e.g. Bernoulli & Laubscher 1972, Zimmerman & Ross 1979, Şengör & Yilmaz 1981) interpret evidence for Cretaceous shallow marine deposition in the Vardar zone and Paleocene–Eocene deformation to indicate a later age of ocean closure. If the latter age is correct, D_1 basement imbrication began prior to final closure of the Vardar ocean basin. Whatever the age of continental collision, blueschist facies metamorphism and deformation of continental crust occurred from ~60 until <40 Ma in the Olympos region and temperatures decreased with time as lower structural levels were deformed. Even though temperatures were low (<250–350°C), both the crystalline basement rocks and carbonates behaved ductilely. Microstructural evidence suggests higher temperatures of deformation than do metamorphic mineral assemblages. Ductility may have been enhanced by shear heating along the thrust surface, where temperatures appear to have reached 400°C (Barton & England 1979) or by the presence of fluids.

Paleogeographic implications

Deformation in the Mt. Olympos region took place in the context of overall convergence between the Apulian and European plates and the closing of Tethyan Ocean basins from Late Jurassic to Tertiary time. Detailed discussion of the controversy and implications of various paleogeographic configurations is beyond the scope of this paper, nevertheless, it is important to note that the SW-vergence of thrusting of the nappes at Mt. Olympos documented here suggests that the ophiolite nappes were rooted in the Vardar ocean basin to the northeast (Bernoulli & Laubscher 1972, Zimmerman 1972, Mercier *et al.* 1975). This, together with the observation that nappes between the Olympos unit and ophiolite unit are all continental in origin, suggests that the Pelagonian zone formed the leading edge of the Apulian plate and was not separated from the external Hellenides by an ocean basin (e.g. Hynes *et al.* 1972; see summary in Robertson & Dixon 1984).

Significance of D_5 *and* D_7 *normal faulting*

There is a discrepancy between the amount of extension recorded by D_5 and D_7 and the amount necessary to exhume the blueschist facies rocks from >20 km depth. The blueschists may have been moved upward by underplating of more external thrust sheets (e.g. D_4), but low-angle and high-angle normal faults have played an important role in decompression and unroofing. The maximum apparent displacement on D_5 and D_7 normal faults is ~6–8 km, the approximate thickness of the exposed thrust sheets between the ophiolite unit and the Olympos unit. An unknown thickness could have been removed by erosion as clasts of Pelagonian metamorphic rocks are abundant in the Mesohellenic molasse basin west of the Olympos region (Fig. 1). However, there appears to be an insufficient volume of Pelagonian-derived sediment to account for the apparent ~15 km discrepancy (Brunn 1956, Papanikolaou *et al.* 1988) and it is likely there are additional, presently unrecognized normal faults west of the Olympos region.

The identification of low-angle normal faults at the base of the ophiolite unit in the Mt. Olympos region has important implications. Low-angle faults are commonly mapped as thrust faults in the absence of good kinematic

indicators. The early Miocene extensional event identified in the Olympos region may be more widespread and regionally important than previously recognized. The Mesohellenic basin developed during extension that occurred in the upper part of the Eocene–Oligocene thrust belt and east of contemporaneous (Oligo-Miocene) thrusting in the external Hellenides (Papanikolaou *et al.* 1988). It seems likely that low-angle normal faults with significant displacement may occur throughout the Pelagonian zone and perhaps throughout the Hellenides (e.g. Dinter 1991). Only after quantitative estimates of Miocene and younger extension across the Pelagonian zone are made, will meaningful estimates of regional shortening be possible. The 'palinspastic problem' of requiring thrusts with several hundred kilometers of displacement to explain the position of ophiolites in the Hellenides (Bernoulli & Laubscher 1972, Barton 1979) may be resolved with recognition of significant amounts of extension in continental Greece.

Normal faults similar to D_7 faults extend along the western margin of the Vardar zone and bound the mountains of the eastern Pelagonian zone for several hundred kilometers along strike in Yugoslavia and Greece. This extensional deformation uplifted the mountains by at least 3 km (the height of Mt. Olympos) with respect to the adjacent north Aegean basin. Other Quaternary basins subparallel to the Vardar basin occur west of the Olympos region (Schermer 1990).

We are just beginning to realize the significance and characteristics of extension within convergent regimes; this is a long-standing problem in Mediterranean tectonics. Normal faulting closely followed thrust faulting in the Olympos region. In a regional context, D_5–D_7 extension occurred during contemporaneous shortening and progression of deformation toward the foreland documented by the progressive younging of flysch and the age of the youngest rocks deformed in the thrust sheets of the external Hellenides (e.g. Jacobshagen *et al.* 1978). The geometric and kinematic data presented here do not directly constrain whether such extension is the result of the collapse of over-thickened crust (Dalmayrac & Molnar 1981, Royden & Burchfiel 1987) or a result of forces at the plate boundary (e.g. trench rollback; Royden 1987, Royden & Burchfiel 1989). The present-day Hellenic arc and trench system was initiated at ~12 Ma (Le Pichon & Angelier 1979), ~10 Ma later than the beginning of extension in the Mt. Olympos region. The age of early extensional events and the close association in time and space following major crustal shortening suggests that the initiation of extension may have been driven by an overthickened crust. Younger and ongoing extension is more likely related to the modern plate margin regime and may be driven by slab retreat.

CONCLUSIONS

Detailed study of the geometry and kinematics of deformation in the Mt. Olympos region provides the following constraints on the structural evolution of subducted continental crust. (1) Deformation of the leading edge of the Apulian plate (Pelagonian zone) included basement-involved thrusting and continental subduction that may have begun before collision of the Apulian and European plates. (2) Basement gneisses and cover sedimentary rocks were detached in thin (250 m–4 km), complexly folded nappes during foreland-vergent (southwest) thrusting. (3) Extension began shortly after thrusting, excised much of the original nappe stack, and occurred above and east of contemporaneous thrusting in the western Hellenides. (4) The present-day geometry of the nappes is largely controlled by extensional faults, which were partly (but not solely) responsible for exhumation of the blueschist facies rocks.

Acknowledgements—This paper represents part of my Ph.D. dissertation under the direction of B.C. Burchfiel at M.I.T. I thank Clark Burchfiel for guidance during the research; Clark, K. V. Hodges and P. Crowley offered helpful comments on an early version of the paper. I am grateful to B. Cleaver, M. Smith and S. Kruse for field assistance, and to D. Papanikolaou for logistical support in Greece. The work was supported by a National Science Foundation Graduate Fellowship, Sigma Xi Grant-in-Aid of Research, and Geological Society of America research grant to Schermer, and by support from Schlumberger Corporation to B. C. Burchfiel. Manuscript preparation was in part supported by a University of California President's Fellowship and the Geology Department, Western Washington University. G. Mustoe produced the photographic figures and D. Denton drafted the maps. G. Lister, J. Mercier, D. Dietrich and editor P. Hudleston provided extremely helpful reviews.

REFERENCES

Ampferer, O. 1906. Über das Bewegungsbild von Faltengebirgen. *Jb. Geol. Reichsanst* **56**, 539–622.

Aubouin, J. 1959. Contribution a l'étude géologique de la Gréce septentrionale: les confins de l'Epire et de la Thessalia. *Annls géol. Pays Hell.* **10**, 1–483.

Bally, A. W. 1975. A geodynamic scenario for hydrocarbon occurrences. *Proc. 9th World Petrol. Congr. Tokyo* **2**, 33–44.

Bally, A. W. 1981. Thoughts on the tectonics of folded belts. In: *Thrust and Nappe Tectonics* (edited by McClay, K. R. & Price, N. J.). *Spec. Publs geol. Soc. Lond.* **9**, 13–31.

Barton, C. M. 1975. Mount Olympos, Greece: new light on an old window. *J. geol. Soc. Lond.* **131**, 389–396.

Barton, C. M. 1976. The tectonic vector and emplacement age of an allochthonous basement slice in the Olympos area, N. E. Greece, *Bull. Soc. géol. Fr.* **18**, 253–258.

Barton, C. M. 1979. Structural evolution of the Vardar root zone, northern Greece: Discussion and reply. *Bull. geol. Soc. Am.* **90**, 125–126.

Barton, C. M. & England, P. C. 1979. Shear heating at the Olympos (Greece) thrust and the deformation properties of carbonates at geological strain rates. *Bull. geol. Soc. Am.* **90**, 483–492.

Bernoulli, D. & Laubscher, H. 1972. The palinspastic problem of the Hellenides. *Eclog. geol. Helv.* **65**, 107–118.

Brunn, J. H. 1956. Contribution à l'étude geologique du Pinde sepentrional et d'une partie de la Macédoine. *Annls géol. Pays Hell.* **8**, 1–258.

Burchfiel, B. C. 1980. Eastern European Alpine system and the Carpathian orocline as an example of collision tectonics. *Tectonophysics* **63**, 31–61.

Chopin, C. 1984. Coesite and pure pyrope in high-grade blueschists of the Western Alps: a first record and some consequences. *Contr. Miner. Petrol.* **86**, 107–118.

Dalmayrac, B. & Molnar, P. 1981. Parallel thrust and normal faulting in Peru and constraints on the state of stress. *Earth Planet. Sci. Lett.* **55**, 473–481.

Dèrycke, F. & Godfriaux, I. 1976. Métamorphismes schistes bleus et schistes verts dans l'Ossa et le Bas- Olympe (Thessalie-Grèce). *Bull. Soc. géol. Fr.* **18**, 252.

Dèrycke, F. & Godfriaux, I. 1978. Découverte de microfaunes paléogénes dans le flysch métamorphique de Spilia (Ossa, Grèce). *C.r. Acad. Sci., Paris* **286**, 555–558.

Dinter, D. A. 1991. Neogene detachment faulting and the Rhodope metamorphic core complexes, northern Greece. *Eos* **72**, 460.

Escher, A. & Watterson, J. 1974. Stretching fabrics, folds and crustal shortening. *Tectonophysics* **22**, 223–231.

Fleury, J. J. & Godfriaux, I. 1974. Arguments pour l'attribution de la série de la fenêtre de l'Olympe (Grèce) à la zone de Gavrovro-Tripolitza: présence de fossiles du Maestrichtien et de l'Eocène inférieur (et moyen?). *Annls Soc. géol. N.* **94**, 149–156.

Giese, P., Reutter, K.-J., Jacobshagen, V. & Nicolich, R. 1982. Explosion seismic crustal studies in the Alpine-Mediterranean region and their implications to tectonic processes. In *Alpine–Mediterranean Geodynamics. Am. Geophys. Un. Geodyn. Ser.* **7**, 39–74.

Godfriaux, I. 1968. Etude géologique de la région de l'Olympe (Grèce). *Annls géol. Pays Hell.* **19**, 1–271.

Godfriaux, I. 1977. L'Olympe. *Bull. géol. Soc. Fr.* **19**, 45–49.

Godfriaux, I., Ferrière, J. & Schmitt, A. 1988. Le dévelopment en contexte continental d'un métamorphisme HP/BT: Les "schistes bleus" tertiaires Thessaliens. *Bull. geol. Soc. Greece* **20**, 175–192.

Godfriaux, I. & Pichon, J. F. 1980. Sur l'importance des évènements tectoniques et métamorphiques d'âge tertiaire en Thessalie septentrionale (Olympe, Ossa, Flambouron). *Annls. géol. Soc. N.* **99**, 367–376.

Hansen, E. 1966. Methods of deducing slip-line orientations from the geometry of folds. *Ann. Rep. Dir. Geophys. Lab., Wash., DC* **65**, 387–405.

Harland, W. B., Armstrong, R. L., Craig, L. E., Smith, A. G. & Smith, D. G. 1990. *A Geologic Time Scale.* Cambridge University Press, Cambridge.

Hodges, K. V., Bartley, J. M. & Burchfiel, B. C. 1982. Structural evolution of an A-type subduction zone, Lofoten-Rombak area, northern Scandinavian Caledonides. *Tectonics* **1**, 441–462.

Hynes, A. J., Nisbet, E. G., Smith, A. G., Welland, M. J. & Rex, D. C. 1972. Spreading and emplacement ages of some ophiolites in the Othris region (eastern central Greece). *Z. dt geol. Ges.* **123**, 455–468.

Jacobshagen, V., Dürr, S., Kockel, F., Kopp, K. O., Kowalczyk, G., Berckhemer, H. & Büttner, D. 1978. Structure and geodynamic evolution of the Aegean region. In: *Alps, Apennines, Hellenides* (edited by Closs, H., Roeder, D. & Schmidt, K.). E. Schweizerbart'sche Verlagsbuchhandlung, 537–564.

John, B. E. 1987. Geometry and evolution of a mid-crustal extensional fault system; Chemehuevi Mountains, southeastern California. In: *Continental Extensional Tectonics* (edited by Coward, M. P., Dewey, J. F. & Hancock, P. L.). *Spec. Publs geol. Soc. Lond.* **28**, 313–336.

Katsikatsos, G., Migiros, G. & Vidakis, M. 1982. Structure géologique de la région de Thessalie orientale (Gréce). *Annls. géol. Soc. N.* **101**, 177–188.

Le Pichon, X. & Angelier, J. 1979. The Hellenic arc and trench system: A key to the Neotectonic evolution of the eastern Mediterranean area. *Tectonophysics* **60**, 1–42.

Lister, G. S. & Snoke, A. W. 1984. S–C mylonites. *J. Struct. Geol.* **6**, 617–638.

Makris, J. 1977. Geophysical investigations of the Hellenides. *Hamburger Geophys. Einzelschr.* **27**, 98.

Mercier, J. 1968. Étude géologique des zones internes des Hellénides en Macédoine centrale (Grèce). *Annls géol. Pays Hell.* **20**, 1–792.

Mercier, J.-L., Vergély, P. & Bébien, J. 1975. Les ophiolites helléniques "obductées" au Jurassique supérieur sont-elles les vestiges d'un océan téthysien ou d'une mer marginale péri-européenne? *C.r. somm. Séanc. Soc. géol. Fr.* **17**, 108–112.

Migiros, G. 1985. Geologic map of Greece, Gonnoi sheet. Institute for Geology and Mining Research, Athens.

Molnar, P. & Gray, D. 1979. Subduction of continental lithosphere: some constraints and uncertainties. *Geology* **7**, 58–62.

Mountrakis, D., Sapountzis, E., Kilias, A., Eleftheriadis, G. & Christofides, G. 1983. Paleogeographic conditions in the western Pelagonian margin in Greece during the initial rifting of the continental area. *Can. J. Earth Sci.* **20**, 1673–1681.

Nance, D. 1981. Tectonic history of a segment of the Pelagonian zone, northeastern Greece. *Can. J. Earth Sci.* **18**, 1111–1126.

Papanikolaou, D. & Zambetakis-Lekkas. A. 1980. Nouvelles observations et datation de la base de la série pélagonienne (s.s.) dans la région de Kastoria, Gréce. *C.r. Acad. Sci. Paris* **291**, 155–158.

Papanikolaou, D. J. 1984a. An introduction to the geology of Greece: the pre-Alpine units. Department of Geology, University of Athens.

Papanikolaou, D. J. 1984b. The three metamorphic belts of the Hellenides: a review and a kinematic interpretation. In: *The Geological Evolution of the Eastern Mediterranean* (edited by Dixon, J. E. & Robertson, A. H. F.). *Spec. Publs geol. Soc. Lond.* **13**, 649–659.

Papanikolaou, D. J., Lekkas, E., Mariolakis, I. & Mirkou, R. 1988. Geodynamic evolution of the Mesohellenic basin. *Bull. geol. Soc. Greece* **20**, 17–36.

Ramsay, J. G. 1967. *Folding and Fracturing of Rocks.* McGraw-Hill, New York.

Robertson, A. H. F. & Dixon, J. E. 1984. Introduction: aspects of the geological evolution of the Eastern Mediterranean. In: *The Geological Evolution of the Eastern Mediterranean* (edited by Dixon, J. E. & Robertson, A. H. F.). *Spec. Publs geol. Soc. Lond.* **17**, 1–74.

Royden, L. & Burchfiel, B. C. 1989. Are systematic variations in thrust belt style related to plate boundary processes? (The Western Alps versus the Carpathians). *Tectonics* **8**, 51–62.

Royden, L. H. 1987. Segmentation and configuration of subducted lithosphere in Italy: An important control on thrust belt and foredeep evolution. *Geology* **15**, 714–717.

Royden, L. H. & Burchfiel, B. C. 1987. Thin-skinned N–S extension within the convergent Himalayan region: gravitational collapse of a Miocene topographic front. In: *Continental Extensional Tectonics* (edited by Coward, M. P., Dewey, J. F. & Hancock, P. L.). *Spec. Publs geol. Soc. Lond.* **28**, 611–619.

Royse, F., Warner, M. A. & Reese, D. C. 1975. Thrust belt structural geometry and related stratigraphic problems, Wyoming–Idaho–northern Utah. *Rocky Mountain Ass. Geol. Symp. Deep Drilling Frontiers in Central Rocky Mountains,* 41–54.

Schermer, E. R. 1989. Tectonic evolution of the Mt. Olympos region, Greece. Unpublished Ph.D. dissertation, Massachusetts Institute of Technology.

Schermer, E. R. 1990. Mechanisms of blueschist creation and preservation in an A-type subduction zone, Mount Olympos region, Greece. *Geology* **18**, 1130–1133.

Schermer, E. R., Lux, D. & Burchfiel, B. C. 1989. Age and tectonic significance of metamorphic events in the Mt. Olympos region, Greece. *Bull. geol. Soc. Greece* **23**, 13–27.

Schermer, E. R., Lux, D. R. & Burchfiel, B. C. 1990. Temperature-time history of subducted continental crust, Mt. Olympos region, Greece. *Tectonics* **9**, 1165–1195.

Schmitt, A. 1983. Nouvelles contributions a l'étude géologique des Pieria, de l'Olympe, et de l'Ossa (Gréce du Nord). Unpublished thèse d'état, Faculté Polytechnique de Mons.

Şengör, C. A. M. & Yilmaz, Y. 1981. Tethyan evolution of Turkey: a plate tectonic approach. *Tectonophysics* **75**, 181–241.

Simpson, C. & De Paor, D. 1991. Deformation and kinematics of high strain zones. *Geol. Soc. Am. Short Course Notes.*

Simpson, C. & Schmid, S. M. 1983. Microstructural indicators of sense of shear in shear zones. *Bull. geol. Soc. Am.* **94**, 1281–1288.

Smith, A. G. 1971. Alpine deformation and the oceanic areas of the Tethys, Mediterranean and Atlantic. *Bull. geol. Soc. Am.* **82**, 2039–2070.

Smith, A. G., Hynes, A. J., Menzies, M., Nisbet, E. G., Price, I., Welland, M. J. P. & Ferriére, J. 1975. The stratigraphy of the Othris mountains, eastern central Greece: a deformed Mesozoic continental margin sequence. *Eclog. geol. Helv.* **68**, 463–481.

Vergély, P. 1976. Chevauchement vers l'Ouest et rétrocharriage vers l'Est des ophiolites: deux phases tectoniques au cours du Jurassique supérieur-Éocrétacé dans les Hellénides internes. *Bull. Soc. géol. Fr.* **18**, 231–244.

Vergély, P. 1984. Tectonique des ophiolites dans les Hellénides internes: conséquences sur l'évolution des régions Téthysiennes occidentales. Unpublished Docteur d'Etat, Université de Paris-Sud.

Vergély, P. & Mercier, J. 1990. La fenêtre métamorphique de l'Olympe (Macédoine, Grèce); Compression et extension cénozoïques. *Bull. Soc. géol. Fr.* **6**, 819–829.

Yarwood, G. A. & Aftalion, M. 1976. Field relations and U–Pb geochronology of a granite from the Pelagonian zone of the Hellenides (High Pieria, Greece). *Bull. Soc. géol. Fr.* **18**, 259–264.

Yarwood, G. A. & Dixon, J. E. 1977. Lower Cretaceous and younger thrusting in the Pelagonian rocks of the High Pieria, Greece. *Sixth Colloq. Aegean Region, Athens,* 269–280.

Zimmerman, J., Jr. 1972. Emplacement of the Vourinos ophiolitic complex, northern Greece. In: *Studies in Earth and Space Sciences* (edited by Shagam, R. *et al.*). *Mem. geol. Soc. Am.* **132**, 225–239.

Zimmerman, J., Jr. & Ross, J. V. 1976. Structural evolution of the Vardar root zone, northern Greece: Discussion and reply. *Bull. geol. Soc. Am.* **90**, 126–128.